Nano Materials Science xxx (xxxx) xxx

Contents lists available at ScienceDirect

Nano Materials Science

journal homepage: www.keaipublishing.com/cn/journals/nano-materials-science/

A comparative study of polymer nanocomposites containing multi-walled carbon nanotubes and graphene nanoplatelets

Xiao Su [a,1], Ruoyu Wang [a,1], Xiaofeng Li [b], Sherif Araby [d], Hsu-Chiang Kuan [b,c], Mohannad Naeem [a], Jun Ma [a,*]

[a] University of South Australia, UniSA STEM and Future Industries Institute, Mawson Lakes, SA, 5095, Australia
[b] College of Materials Science and Engineering, Beijing University of Chemical Technology, Beijing, 100029, China
[c] Department of Energy Application Engineering, Far East University, Tainan County, 744, Taiwan
[d] School of Engineering and Digital Sciences, Nazarbayev University, Nur-Sultan, 010000, Kazakhstan

ARTICLE INFO

Keywords:
Graphene (nano) platelets (GNPs)
Multi-walled carbon nanotubes (MWCNTs)
Polymer nanocomposites
Synergistic effect

ABSTRACT

Featuring exceptional mechanical and functional performance, MWCNTs and graphene (nano)platelets (GNPs or GnPs; each platelet below 10 nm in thickness) have been increasingly used for the development of polymer nanocomposites. Since MWCNTs are now cost-effective at US$30 per kg for industrial applications, this work starts by briefly reviewing the disentanglement and surface modification of MWCNTs as well as the properties of the resulting polymer nanocomposites. GNPs can be made through the thermal treatment of graphite intercalation compounds followed by ultrasonication; GNPs would have lower cost yet higher electrical conductivity over 1,400 S cm^{-1} than MWCNTs. Through proper surface modification and compounding techniques, both types of fillers can reinforce or toughen polymers and simultaneously add anti-static performance. A high ratio of MWCNTs to GNPs would increase the synergy for polymers. Green, solvent-free systhesis methods are desired for polymer nanocomposites. Perspectives on the limitations, current challenges and future prospects are provided.

1. Introduction

Since covalently bonded macromolecules were first identified as "a polymer" by Staudinger et al. in 1920 [1], polymers have demonstrated increasing importance in a broad range of research fields and industrial sectors. However, most pristine polymers lack either stiffness or ductility, let alone electrical and thermal conductivity; their mechanical properties in many cases are unsatisfactory in comparison with metals or ceramics. Therefore, polymer nanocomposites have been developed by compounding fillers into host polymeric matrices. Polymer nanocomposites containing graphene nanoplatelets (GNPs; each below 10 nm in thickness) and MWCNTs are widely researched for many applications. Polymer/GNP nanocomposites are popular in research fields and industrial sectors such as antibacterial, photocatalytic and wastewater treatments. Polymer nanocomposites containing MWCNTs and GNPs are researched towards applications for lithium-air batteries, supercapacitors, wearable devices, adsorption of organic compounds, polyelectrolyte complex membranes, electromagnetic interference shielding, medical hydrogels, and so on [2–6]. Recently reported polymer/GNP/MWCNT nanocomposites can be utilized in many areas, including but not limited to aerospace, flame retarding and electromagnetic interference shielding [7–13].

Based on the rule of mixtures (details to be discussed in *Section* 2.2), the fillers utilized should have high stiffness and aspect ratio. Under mechanical stress, these fillers share a fraction of load through stress transfer across the interface, hence improving the mechanical properties of the matrices. Micron-sized fillers such as metallic fibres and ceramic particles at 15–60 vol% are often needed to improve the properties of host polymers. Using nanofillers often results in a much lower filler fraction usually below 2 vol% for significant improvements to the matrix polymers. Of all the nanofillers reported to-date, graphene and CNTs have attracted extraordinary interests. According to the Clarivate Analytic database, the numbers of publications by keywords of "graphene composites", "CNT composites" and "graphene CNT composites" reveal growing trends over the past 20 years (Fig. 1a&b). Similar numbers of publications are seen for two groups of nanocomposites respectively containing graphene and CNTs from 2010 to 2013, but since 2014 graphene composites have attracted far more interests. Noteworthy is that the studies of polymers containing MWCNTs and graphene appear to

* Corresponding author.
E-mail address: Jun.Ma@unisa.edu.au (J. Ma).
[1] These authors contributed equally to this work.

https://doi.org/10.1016/j.nanoms.2021.08.003
Received 21 May 2021; Accepted 9 August 2021
Available online xxxx

List of symbols and abbreviations

2D	Two dimensional
3D	Three dimensional
CNTs	Carbon nanotubes
SWCNTs	Single-walled carbon nanotubes
MWCNTs	Multi-walled carbon nanotubes
CVD	Chemical vapour deposition
GIC	Graphite intercalation compound
GO	Graphene oxide
GNPs	Graphene nanoplatelets
min	Minute

have just started, and these should be more extensively investigated in the years to come [14–22].

Since reported by Iijima et al. in 1991 [23,24], CNTs have been on the forefront of polymer nanocomposite research. The tubes have covalently bonded structure, high stiffness and strength yet certain flexibility. More importantly, CNTs have higher thermal and electrical conductivity than conventional filler such as carbon fibre and glass fibre; these unique properties make CNTs superior. The team led by Liqun Zhang at Beijing University of Chemical Technology have conducted extensive research of using MWCNTs for elastomers. They found that MWCNT bundles with the same alignment, orientation and reasonable surface defects for each tube can be directly incorporated into an elastomer matrix through melt compounding, inducing a relatively uniform filler dispersion and strong interfacial interactions due to silane-coupling. The resulting nanocomposites demonstrated high mechanical properties, thermal conductivity and antistatic performance. Through further scale-up, the nanocomposites demonstrated the most optimized comprehensive performance for automobile tyres, e.g. fuel efficiency and fatigue resistance [25].

Graphene, as first mechanically exfoliated from graphite by Geim and Novoselov in 2004 [26], is a single atomic layer of sp2 hybridized carbon atoms arranged in a hexagonal lattice. In a graphene sheet, each carbon atom contributes three of its four outer-shell electrons by hybridizing to form σ-bonds with three adjacent atoms in the sheet. The remaining electron contributes to a conduction band that extends over the whole sheet, which provides graphene with semi-metallic characteristics, explaining high stiffness, strength and electrical and thermal conductivity [27–31].

Referring to graphene that is oxidized by strong oxidizers and acids, graphene oxide is electrically insulating; it is prepared from graphite oxide consisting of carbon, oxygen and hydrogen in varying concentrations. Reduced graphene oxide means graphene oxide that is reduced by chemical reactions or thermal treatments, to remove oxygen atoms and to partially recover the conduction band over each sheet. Chemically modified graphene means graphene that is modified by chemical reactions, to obtain solubility or compatibility with polymer or other specific functions; chemically modified graphene in many cases is actually surface-modified, partially oxidized graphene. Other derivatives of graphene may include few-layer graphene and multi-layer graphene.

Few-layer graphene is actually graphene (nano)platelets (GNPs or GnPs; each platelet below 10 nm in thickness). We now distinguish graphene nanoplatelets and nanosheets. Graphene nanosheets usually refer to monolayer or few-layer graphene who must have large lateral dimension, in comparison with the small lateral dimension of GNPs. In polymer processing, GNPs would be preferred over graphene nanosheets because (i) nanosheets are difficult to exfoliate and disperse in polymer melts and (ii) such a large lateral dimension cannot be fully utilized for reinforcement or toughening.

Single-layer graphene has properties that approximate single-walled carbon nanotubes (SWCNTs). However, the high manufacturing costs make both SWCNTs and graphene (US$700 per gram and US$1,000 per gram) unideal for polymer processing and the composite industry. Instead, multi-walled carbon nanotubes (MWCNTs) and GNPs, having far lower manufacturing costs (US$30 per kilogram and potentially US$10–20 per kilogram) yet satisfactory mechanical and functional properties, are suitable to engineering applications.

The dispersion as well as the orientation of GNPs is one of the major aspects that determine the physical and mechanical properties of the resulting polymer nanocomposites. Since polymers and GNPs have vastly different composition and properties, GNPs tend to stack in all polymer matrices, leading to poor dispersion. These platelets generally need to be exfoliated with relatively uniform dispersion in the matrices, and orientation is preferred in some cases. Theoretical research shows that the aligned graphene sheets in an epoxy matrix can markedly increase the electrical conductivity from 3×10^{-12} to 7.5×10^{-6} S·cm^{-1} [32]. Kandare et al. prepared an epoxy/GNP/carbon fibre laminate where GNPs were aligned in the matrix, delivering a 55% higher through-thickness electrical conductivity in comparison with a carbon/epoxy laminate [33].

Without relatively uniform dispersion and controllable interaction with the matrices, however, MWCNTs and GNPs would contribute little to the resulting nanocomposite performance. Since the dispersion and interfacial interactions are mainly determined during the preparation, we will briefly review three common preparation methods, i.e. *in-situ* polymerization, solution mixing and melt compounding. An extensive review was provided by Kaseem et al. [34].

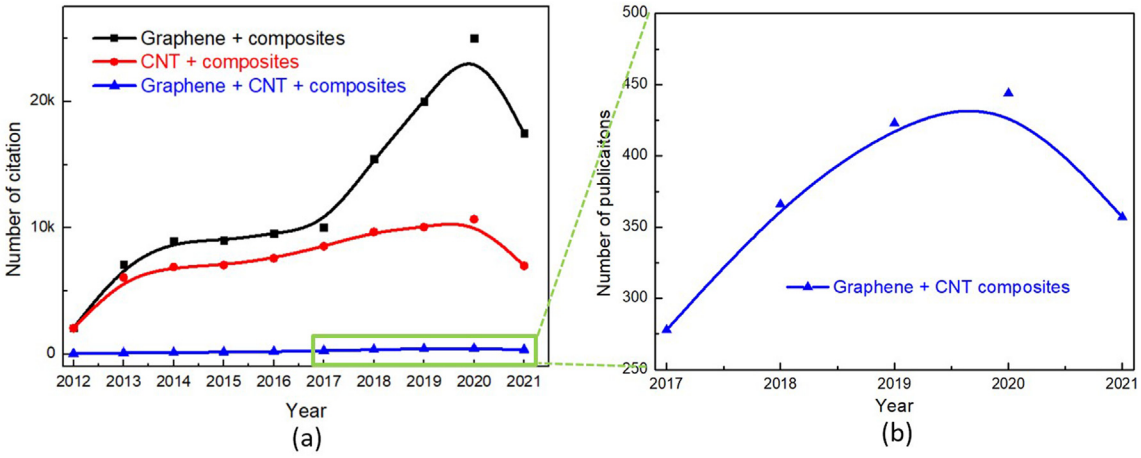

Fig. 1. (a) Number of publications by keywords "carbon nanotubes", "graphene" and "composites" in the title search in 2012–2021 (Clarivate Analytic database; as of July 2021), and (b) publications for "carbon nanotube graphene composites" from 2017 to 2021.

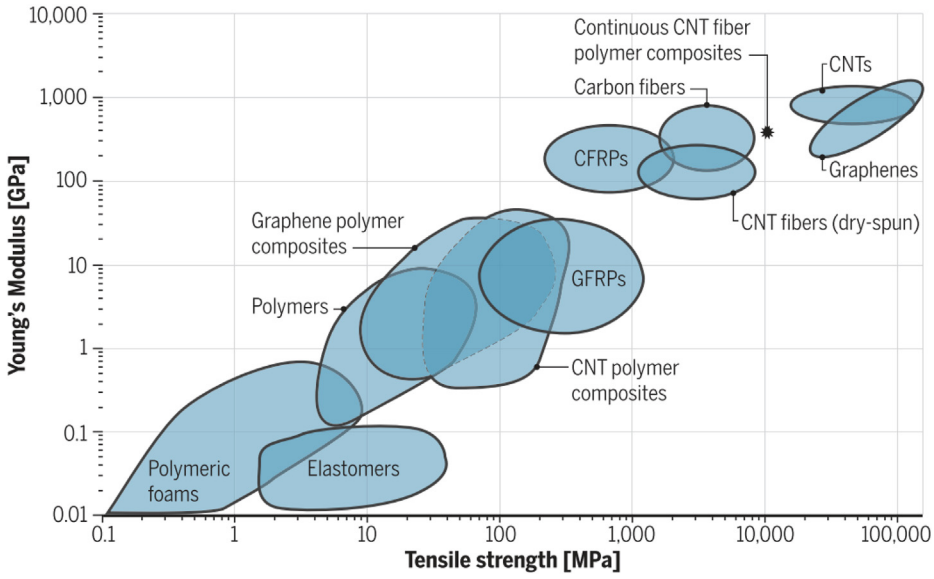

Fig. 2. Ashby plot of Young's modulus against tensile strength for polymer composites and nanocomposites, reprinted with permission from Ref. [54], copyright 2018 Science.

1.1. Preparation of polymer nanocomposites

In-situ polymerization is especially effective in dispersing nanosheets such as GNPs in polymer matrices. The first step is to disperse nanofillers uniformly in monomer solution. After applying heat or radiation, monomers polymerize in the presence of nanofillers. The polymerization may increase the interlayer spacing of nanosheets, thus promoting their exfoliation and dispersion [35]. *In-situ* polymerization is widely researched for epoxy, poly (methyl methacrylate), polystyrene and polyvinyl acetate [36–38]. However, it is not suitable for other polymers, such as elastomers which must have high molecular weight, because nanofillers may cause a steric effect of preventing the growth of

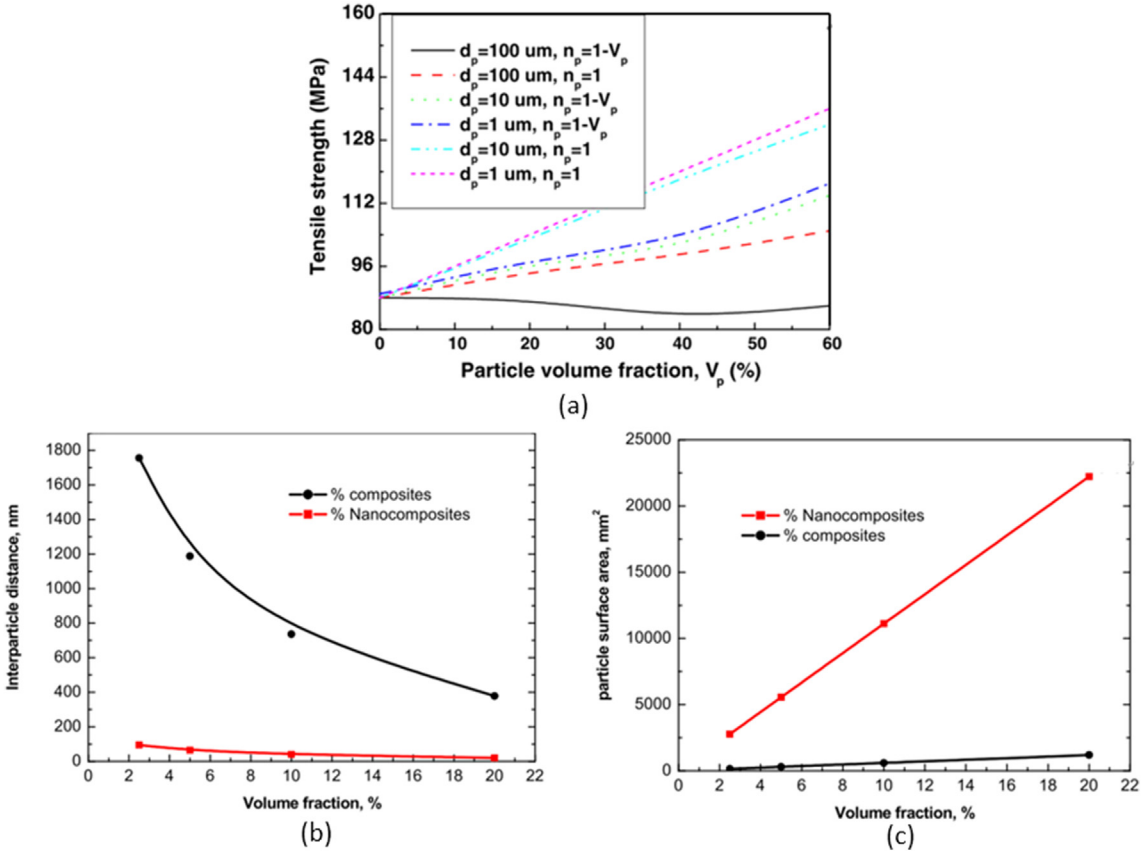

Fig. 3. (a) Effect of particle size on tensile strength for polymer composites, reprinted with permission from Ref. [62], copyright 2001 Elsevier, (b) comparison of interparticle distance between the micron-sized filler and the nano-sized filler, and (c) comparison of total particle surface, reprinted with permission from Ref. [63], copyright 2010 Elsevier.

long-chain molecules in polymerization.

Solution mixing can effectively promote the dispersion of nanofillers within polymers by using a proper solvent. However, this method is not suitable to some thermoplastics such as nylon. Different to *in-situ* polymerization, solution mixing usually needs to dissolve a polymer in a solvent together with nanofillers [39–41]. This method can provide better filler dispersion in the matrix compared with melt compounding [42]. Through mechanical stirring and ultrasonication, nanofillers should achieve relatively uniform dispersion within a polymer solution. After evaporating the solvent, polymer chains may wrap around the fillers embedding those fillers within the matrices [43].

In comparison with *in-situ* polymerization and solution mixing, melt compounding is more favoured in industry due to cost-effectiveness. Fillers are directly mixed with molten polymers by high-degree shearing which can shear-split those aggregated nanoparticles or stacked nanosheets into smaller bundles [44,45]. The commonly used facilities include (i) two-roll mills and internal mixers for elastomers [46,47] and (ii) extrusion and injection moulding facilities for thermoplastics [48]. Since no solvent is involved in melt compounding, this method has become the most practical approach for the mass production of polymer nanocomposites [49–52]. However, melt compounding may cause damage to the fillers' aspect ratio, especially CNTs whose length could be severely reduced [53].

1.2. Why chooses nanomaterials

The Ashby plot in Fig. 2 compares the mechanical properties of polymer nanocomposites based on MWCNTs and GNPs with those conventional composites, i.e. glass fibre reinforced plastic (GFRP) and carbon fibre reinforced plastic (CFRP). It is seen that the mechanical properties of both MWCNT and GNP nanocomposites are rated between CFRP and polymers. The comparison applies to those recently reported [54–57]. Although the nanocomposites have lower mechanical strength than CFRP, the former have higher fracture strain. MWCNT fibres made by dry spun have higher mechanical properties than carbon fibres, indicating that MWCNT fibres have potential to compete with carbon fibres in the near future due to their ultralight yet super strong structures.

So why the nanosized fillers provide polymers with exceptional reinforcing or toughening performance? Filler size was reported for a direct impact on the mechanical behaviour of composites [58–61]. Fig. 3a shows the increment of tensile strength with the reduction of particle size at the same filler fraction [62]. Both the surface-to-surface interparticle distance and the total surface area of fillers pose a direct impact on the strengthening performance of fillers for polymers [63]. The following equations are proposed to highlight the superiority of nanoparticles over conventional micron-sized fillers. In a given volume, the total number N of spherical fillers is Eq 1

$$N = \frac{V \times a}{\frac{4}{3}\pi \times r^3} \tag{1}$$

where V is the total volume, a is the particle fraction, and r is the particle radius. Assuming the same number of identical cubes which exactly fill up the volume V, the lateral size L of the cubes is Eq 2

$$L = r \times \sqrt[3]{\frac{4}{3a}\pi} \tag{2}$$

The surface-surface interparticle distance of adjacent nanoparticles ΔL is the difference between the lateral size of the cube and the diameter of the particle Eq 3:

$$\Delta L = r \times \sqrt[3]{\frac{4}{3a}\pi} - 2r = r \times \left(\sqrt[3]{\frac{4\pi}{3a}} - 2\right) \tag{3}$$

And the total particle surface area S in volume V is Eq 4

$$S = 4\pi \times r^2 \times \frac{V \times a}{\frac{4}{3}\pi \times r^3} = \frac{3a}{r}V \tag{4}$$

For cylindrical fillers such as MWCNTs, the total filler number N is Eq 5

$$N = \frac{V \times a}{\pi \times r^2 \times h} \tag{5}$$

where V is the total volume, a is the MWCNT fraction, r is the radius of each MWCNT, and h is the MWCNT length. By assuming trivial end surface, the total external MWCNT surface area S in a volume V is Eq 6

$$S = 2\pi r \times h \times \frac{V \times a}{\pi \times r^2 \times h} = \frac{2a}{r}V \tag{6}$$

For 2D fillers such as GNPs, the total filler number N is Eq 7

$$N = \frac{V \times a}{r^2 \times t} \tag{7}$$

where V is the total volume, a is the GNP fraction, r is the lateral size of GNPs, and t is the thickness. By assuming trivial thickness, the total GNP surface area S in a volume V is Eq 8

$$S = 2 \times r^2 \times \frac{V \times a}{r^2 \times t} = 2\frac{a}{t}V \tag{8}$$

The calculated data by Equations (3) and (4) are plotted in Fig. 3b&c, where the surface-surface interparticle distance in composites obviously reduces with the fractions, and the interparticle distances in nanocomposites are substantially lower [62]. With such low interparticle distances, nanoparticles at a substantially low fraction can interact with each other far more efficiently than microparticles, to reinforce the matrix or initiate those matrix toughening mechanisms such as shear banding. In Fig. 3b, the total surface area of nanoparticles increases significantly with volume fractions compared to those in composites, implying that nanoparticles are able to interact with the matrix far more efficiently to promote matrix deformation for absorption of fracture energy [62]. As a result, nanocomposites should demonstrate a much higher reinforcing or toughening effect at a low particle fraction than conventional composites. In Fig. 3c, the total surface area of nanoparticles increases significantly with the volume fractions in comparison with micron-sized fillers, which provides more-interface interactions between the filler and the matrix in the case of uniform dispersion. Thus, nanoscale fillers can share more mechanical loading from the matrix, implying a stronger reinforcing or toughening effect [63].

In summary, these mathematical models provide theoretical support to selecting nanoscale fillers over their micron-sized peers. Nanofillers are now competing with and have potential to replace some conventional fillers in engineering practice.

2. Carbon nanotubes

Carbon nanotubes (CNTs) have seamless hexagonal honeycomb lattices similar to graphene, and their unique cylindrical structure can be treated as rolled-up graphene sheets. CNTs are usually considered as one-dimensional materials. According to the number of cylinder walls, CNTs are classified into single-walled CNTs (SWCNTs) and multi-walled CNTs (MWCNTs).

SWCNTs each have a diameter of 1.0 ± 0.2 nm [64,65]. Each MWCNT has two or more concentric cylindrical shells which coaxially form around a central hollow core by van der Waals forces between adjacent shells, with an average inter-sheet distance of ~0.34 nm similar to graphite. The outer diameter of MWCNTs ranges 5–50 nm and their length ranges from 100 nm to several centimetres depending on the preparation conditions [66,67]. The cylindrical, multi-layer structure of MWCNTs makes them good candidates to bridge polymer macromolecules in host matrices and thus to improve the performance of the

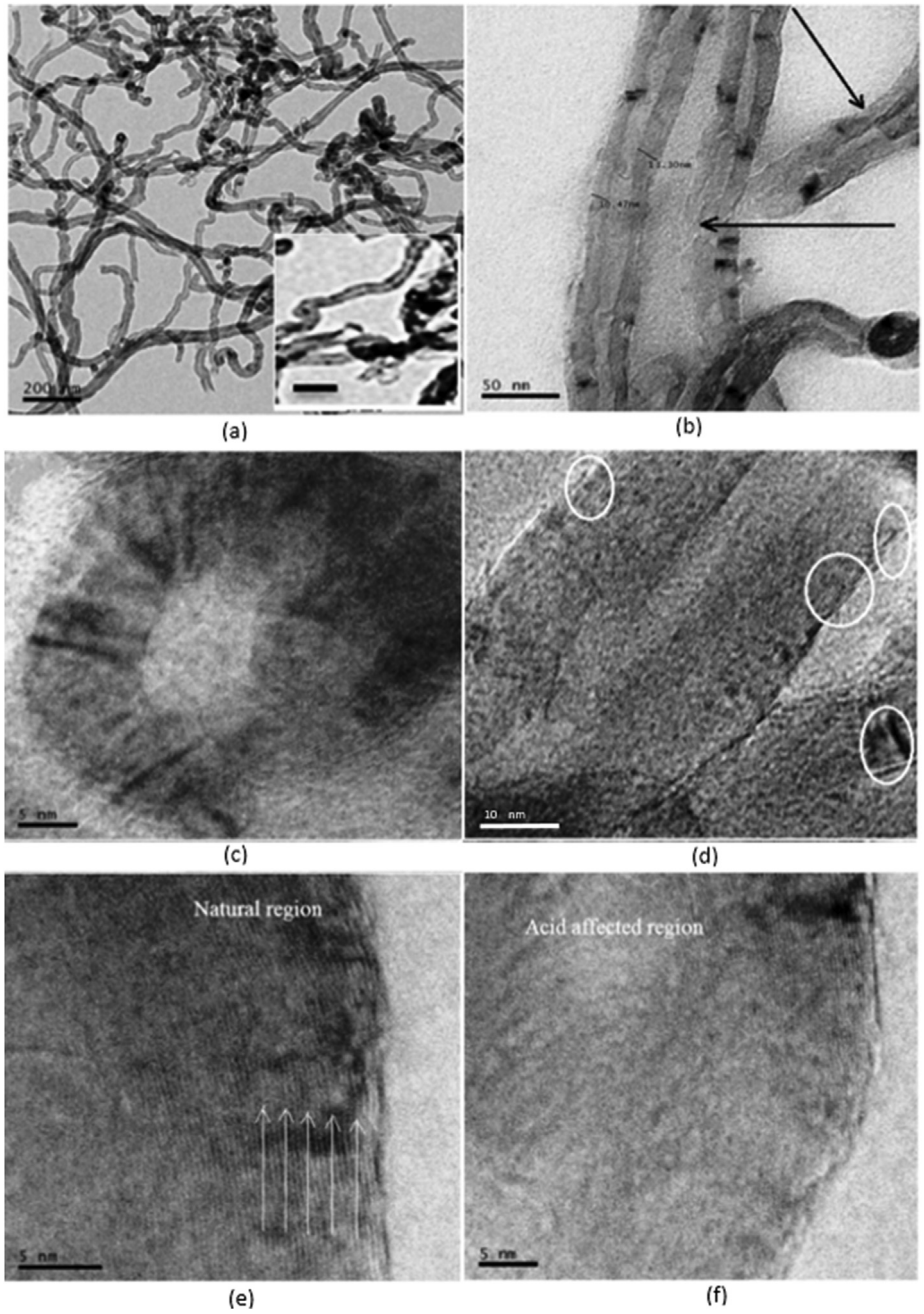

Fig. 4. (a and its insert) pristine MWCNTs, (b) black arrows indicate that side wall has been damaged, (c) open end cap of a modified MWCNT, (d) circles indicate the defects on the modified MWCNTs, (e) white arrows indicate the side wall edge, and (f) side wall is partially destroyed, reprinted with permission from Ref. [72], copyright 2018 Elsevier.

resulting nanocomposites [68]. Hence, incorporating MWCNTs into polymers has drawn considerable attention in both academia and industry. However, the challenge of dispersing as-produced MWCNTs in polymers has severely tarnished the expected reinforcing performance. This is mainly due to both densely entangled bundles and poor interactions between MWCNTs and the host matrices [69]. Approaches to solving the problems are discussed below.

2.1. Disentanglement and surface modification of MWCNTs

Commercially available MWCNTs usually hold in large bundles by van der Waals forces, and each bundle contains fifty to a few hundreds of individual tubes [70]. If directly mixing raw MWCNTs (heavily entangled) with pristine polymers, these bundles would act as defects causing stress concentration within polymer matrices, which would obstruct the expected mechanical and electrical performance of the resulting nanocomposites. Thus, it is essential to disentangle MWCNTs before compounding with polymers. In this regards, there are four most commonly used methods: ultrasonication, calendaring, ball milling and stirring.

Similar to conventional polymer composites where compatibility is key to the performance [71], chemical surface modification aims to build up covalent bonds between organic molecules and MWCNTs. Direct covalent and defect surface modification are the two most widely used approaches: the direct covalent approach turns sp^2 bonds into sp^3 bonds making MWCNTs insulative due to loss of π-conjunction, and the defect surface modification creates carboxylic (–COOH) and hydroxyl (–OH) groups by acidic oxidation. TEM micrographs in Fig. 4 display the structure of MWCNTs before and after chemical oxidation. The dark lines

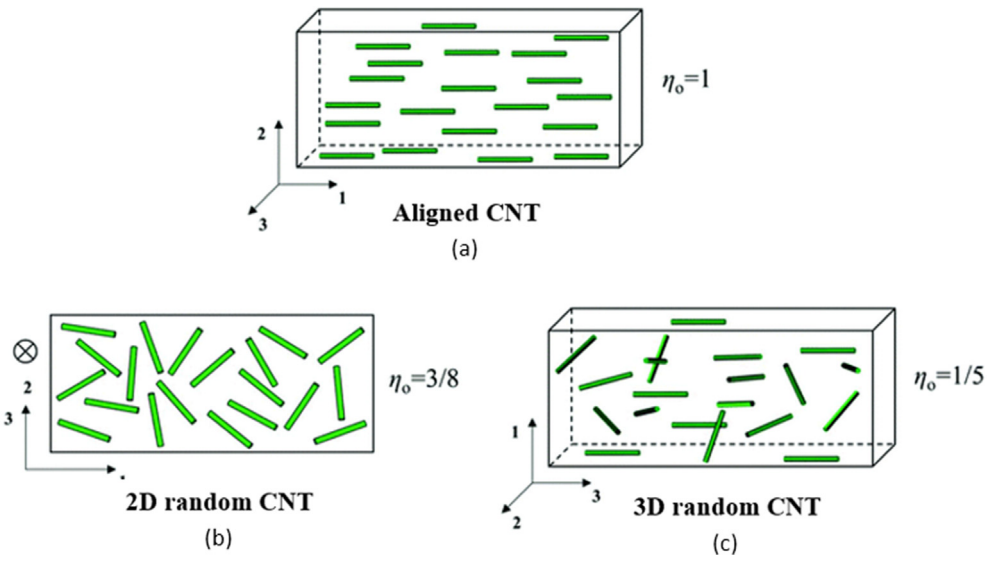

Fig. 5. Schematics of MWCNT nanocomposites with different filler orientations: (a) aligned, (b) randomly oriented in-plane, and (c) 3D randomly oriented, reprinted with permission from Ref. [87], copyright Royal 2020 Society of Chemistry.

marked by white arrows refer to the edges of nanotube sidewalls (Fig. 4e). This lattice fringe displays a 0.34 nm interlayer spacing of nanotube sidewalls. The dark lines observed in Fig. 4e are disappeared in Fig. 4f due to the chemical oxidation which has turned the crystalline sidewalls into amorphous [72]. The chemical surface modification converts the hydrophobic MWCNT surface into hydrophilic, which improves their dispersion status in some solvents and polymer matrices but reduces their conductivity [73,74].

Surface modification by physical means such as surfactant adsorption aims to change the surface condition of nanotubes without damaging their structure [75–77]. Polymer wrapping uses macromolecules such as poly (*p*-phenylene vinylene) or polystyrene to wrap around the MWCNT sidewalls by van der Waals and π–π stacking, which are effective in improving the dispersion of MWCNTs in polymeric matrices [78]. However, the wrapped polymers can severely reduce the conductivity of MWCNTs. Meanwhile, the surfactant adsorption approach uses surfactants, such as octyl phenyl ether (Triton X-100) or dodecyl trimethyl ammonium bromide, to reduce the surface tension of MWCNTs, which prevents them from aggregating [79]. Noteworthy is that these surfactants are suitable to certain polymers but not to others.

2.2. Mechanism of MWCNTs reinforcing polymers

Theoretical studies have been undertaken since early 90s to understand the reinforcing mechanisms of fibre-reinforced polymers, which provided guidance to the development of polymer/MWCNT nanocomposites [80–88]. Among these sophisticated mechanisms/models, we summarized two most relevant – the rule of mixtures and the Halpin-Tsai model – to discuss the strengthening effect of MWCNTs in polymer nanocomposites.

The rule of mixture model is the simplest, which considers that (i) the matrix is isotropic and elastic and (ii) MWCNTs are elastic and they can align and extend along the entire specimen. Assuming that the MWCNTs are well attached to the system with stress applied in the tube alignment direction, both matrix and fillers can be equally strained. In this case, the nanocomposite tensile modulus Y_c in the alignment direction is obtained by Eq 9:

$$Y_c = (Y_f - Y_m)V_f + Y_m \tag{9}$$

where Y_c, Y_f,Y_m and V_f are nanocomposite modulus, filler modulus and matrix modulus and filler volume fraction, respectively [80].

However, this model is not appropriate for those fillers which are much shorter than the specimen, especially nanoscale fillers such as MWCNTs. Therefore, we shall take into account the matrix-filler stress transfer. Under loading, the maximum stress transferred to the fillers is described by the interfacial stress transfer τ. Since the stress scales with filler length l, the stress transferred at certain critical length l_c should be sufficient to break the filler. The critical length for a hollow cylinder is Eq 10:

$$l_c = \frac{\sigma_f D}{2\tau}\left[1 - \frac{D_i^2}{D^2}\right] \tag{10}$$

where σ_f and τ are the fibre strength and interfacial stress transfer, and D and D_i are the filler external and internal diameters. From the equation, we can see that σ_f increases with l_c, which means long fillers carrying loads more efficiently than short fillers. This concept first raised in the Cox–Krenchel model was further modified to calculate the modulus of a composite with aligned fillers Eq 11 [80]:

$$Y_c = (\eta_l Y_f - Y_m)V_f + Y_m \tag{11}$$

wwhere η_l is the length efficiency factor Eq 12 and Eq 13,

$$\eta_l = 1 - \frac{Tanh(a \cdot l/D)}{a \cdot l/D} \tag{12}$$

$$a = \sqrt{\frac{-3Y_m}{2Y_f lnV_f}} \tag{13}$$

From the equation, the length efficiency factor approaches 1 when $l/D \geq 10$, which indicates that the fillers having a high aspect ratio (length-to-width ratio) would perform better in the composites.

In other cases where fillers are not aligned within the matrix, the modulus can be concluded as Eq 14:

$$Y_c = (\eta_0 \eta_l Y_f - Y_m)V_f + Y_m \tag{14}$$

where η_0 is the orientation efficiency factor. As shown in Fig. 5, for aligned fillers, η_0 equals 1; for fillers aligned in a plane, η_0 equals 3/8; and for randomly oriented fillers, η_0 equals 1/5 .

A similar equation can be derived to compute composite strength. For very long aligned fillers ($l > \sim 10 l_c$), the strength is obtained by Eq 15:

Table 1
Mechanical properties of polymer/MWCNT nanocomposites.

Matrix	Filler Type	Filler Fraction (wt%)	Young's Modulus (GPa); polymers	Tensile Strength (MPa); polymers	Young's Modulus (GPa) and increment (%); composites	Tensile Strength (MPa) and increment (%); composites	Ref.
Polyester	Pristine MWCNTs	0.05	2.32	25.5	2.39 (3.0%)	27.0 (5.9%)	[94]
Polyimides	Pristine MWCNTs	2	1.37	45.8	1.65 (20.4%)	73.6 (60.7%)	[95]
Epoxy	Pristine MWCNTs	0.5	2.90	60.9	3.13 (7.93%)	67.9 (11.5%)	[96]
PC	Pristine MWCNTs	2	1.38	66.5	1.57 (13.8%)	79.6 (19.7%)	[101]
PA	Modified MWCNTs	8	1.86	57.0	2.84 (52.7%)	62.0 (8.8%)	[102]
PMMA	Pristine MWCNTs	10	2.07	12.8	3.65 (76.3%)	23.9 (86.7%)	[103]
PP	Pristine MWCNTs	8	0.81	29.4	1.19 (46.9%)	31.9 (8.5%)	[104]
HDPE	Pristine MWCNTs	2.5	0.75	26	1.18 (57.3%)	34 (30.8%)	[105]

$$\sigma_c = (\sigma_f - \sigma_m)V_f + \sigma_m \tag{15}$$

where σ_c is the composite strength, σ_f is the filler strength, and σ_m is the matrix strength. Similar to modulus, the composite strength reduces when fillers become shorter. For medium-length fillers ($l > l_c$) the composite strength is Eq 16:

$$\sigma_c = (\eta_s\sigma_f - \sigma_m)V_f + \sigma_m \tag{16}$$

where η_s is the strength efficiency factor, given by $\eta_s=(l\text{-}l_c/2l)$. When $l > l_c$, the fillers break under applied stress. When $l < l_c$, stress applied to the system cannot be sufficiently transferred to the fillers; on the contrary, fillers are pulled out from the matrix. If this is the case, then the strength is Eq 17:

$$\sigma_c = (\tau l / D - \sigma_m)V_f + \sigma_m \tag{17}$$

This equation describes the situation where fillers are pulled out of the system; thus, the strength is controlled by the interface strength τ between the filler and the matrix, instead of the filler strength.

The Halpin-Tsai model is a well-known model developed basically for continuous fibre composites. In aligned fibre composites, the Halpin-Tsai model describes modulus of elasticity as Eq 18 [89–91]:

$$Y_c = Y_m\frac{(1+\xi\eta V_f)}{(1-\eta V_f)} \tag{18}$$

where $\xi = 2l/D$ and Eq 19

$$\eta = \frac{Y_f/Y_m - 1}{Y_f/Y_m + 1} \tag{19}$$

And for randomly oriented composites, it is written as Eq 20 and 21

$$\frac{Y_c}{Y_m} = \frac{3}{8}\left[\frac{1+\xi\eta_L V_f}{1-\eta_L V_f}\right] + \frac{5}{8}\left[\frac{1+2\eta_T V_f}{1-\eta_T V_f}\right] \tag{20}$$

$$Where\ \eta_L = \frac{Y_f/Y_m - 1}{Y_f/Y_m + \xi}\ and\ \eta_T = \frac{Y_f/Y_m - 1}{Y_f/Y_m + 2} \tag{21}$$

The Halpin-Tsai model is precise for composites at low filler fractions, but it lacks accuracy for composites having high filler fractions [92,93].

In summary, both models show that those fillers having a high aspect ratio and strong interfacial strength are advantageous for composite reinforcement. These have provided a solid theoretical support to selecting MWCNTs as the fillers for polymers. However, MWCNTs belong to the short-fibre category, and this limits their performance as flexible fillers within host matrices. Nevertheless, MWCNTs may become a competitive candidate or even replace continuous carbon fibres if these nanotubes can be assembled through a macroscopic scale. The reinforcing mechanisms of different filler geometries in polymer matrices are extensively reviewed by Coleman [80] and Dimitrios [66].

2.2.1. *Mechanical properties*

Cost-effective MWCNTs can dramatically improve the mechanical behaviours of host polymers. This section examines the influence of various parameters (such as polymer matrices, MWCNT modifications, filler fractions and fabrication methods) on the mechanical properties of the resulting nanocomposites.

In Table 1, the structure of host polymers poses a direct impact on the dispersion and performance of MWCNTs. For thermoset polymers such as epoxy resin, polyester resin, polyimides and vinyl ester resin, MWCNTs in many cases provide remarkable enhancement of the mechanical properties. As reported by Shokrieh et al., a polyester/MWCNT nanocomposite at 0.05 wt% showed a 3.0% improvement of Young's modulus and 5.9% for tensile strength [94]. A polyimide/MWCNT composite at 2 wt% was reported for 20.4% and 60.7% improvements in Young's modulus and tensile strength [95]. In Ting et al. work, an epoxy/MWCNT nanocomposite at 0.5 wt% demonstrated fair mechanical properties in comparison with neat epoxy (7.93% higher for Young's modulus and 11.5% for tensile strength) [96]. In addition, the surface modification of MWCNTs by coating with nickel-doped Fe_3O_4 nanocrystals led to microwave absorption [97].

The difference in the mechanical property improvements is explained below. Since pristine MWCNTs have high aspect ratio, smooth surface and vastly different composition to polymers, these tubes reaggregate themselves in matrices during solidification. Introducing functional groups onto MWCNT surface can largely enhance the interaction between MWCNTs and the polymer matrices, which should prevent the reaggregation.

In addition to surface modification, fabrication methods also affect the performance of the resulting nanocomposites. For thermoplastic polymers such as polyethylene (PE), high density polyethylene (HDPE), polyvinyl chloride (PVC), polymethyl methacrylate (PMMA) and polypropylene (PP), melt compounding is more cost-effective than solution mixing. As listed in Table 1, at high filler fractions (>5 wt%), melting compounding can effectively disperse MWCNTs into thermoplastic polymer matrices to attain significant mechanical property improvements. However, it is worth noting that the improvements are rather limited for HDPE nanocomposites in some cases [98], because the high crystalline structure of HDPE limits the dispersion of pristine MWCNTs in the matrix.

According to the data in Table 1, MWCNTs improve the mechanical properties of plastic matrices, whilst their reinforcing efficiency may be

Table 2
Electrical conductivity of polymer/MWCNT nanocomposites.

Matrix	Filler type	Fraction (wt%)	Fabrication method	Composite Conductivity ($S \cdot cm^{-1}$)	Ref.
Epoxy	Pristine MWCNTs	0.5	*In-situ* polymerization	1.0×10^{-6}	[100]
Epoxy	Modified MWCNTs	0.5	*In-situ* polymerization	3.2×10^{-3}	[99]
SBR	Pristine MWCNTs	10	Melt compounding	2.4×10^{-6}	[106]
PC	Modified MWCNTs	2.5	Melt compounding	7.3×10^{-2}	[107]
PA	Modified MWCNTs	8.0	Solution casting	6.0×10^{-1}	[102]
PP	Prinstine MWCNTs	1.8	Melt compounding	8.3×10^{-3}	[108]
PMMA	Pristine MWCNTs	2.2	in-situ polymerization	1.0×10^{-1}	[109]
HDPE	Pristine MWCNTs	4.5	Melt compounding	1.0×10^{-4}	[110]
PLA & HDPE	Pristine MWCNTs	1	Melt compounding	1.0×10^{-6}	[111]

limited for brittle polymers. The mechanisms and properties for various polymer/MWCNT composites are extensively discussed in Kumar's review in 2020 [60].

2.2.2. *Electrical properties*

As one class of the most electrically conductive nanoscale fillers, MWCNTs are able to alter the insulating nature of various polymers. The network formed by MWCNTs provides a free path for electron transport even at a low fraction to make polymers conductive. However, the conductivity is influenced by many factors. This section aims to discuss the influence of MWCNTs on the electrical conductivity of the resultant polymer nanocomposites.

In Table 2, thermoset polymers, e.g. epoxy and styrene-butadiene rubber (SBR), have shown interesting electrical performance once compounded with either pristine or modified MWCNTs. An epoxy/modified MWCNT nanocomposite at 0.5 wt% demonstrates higher conductivity than the unmodified one (i.e. 10^{-3} $S \cdot cm^{-1}$ vs 10^{-6} $S \cdot cm^{-1}$) [99,100]. This means that at low filler fractions, the modified MWCNTs are more likely to form conductive network than pristine MWCNTs within polymer matrices. From our perspectives, this is likely because (i) although the

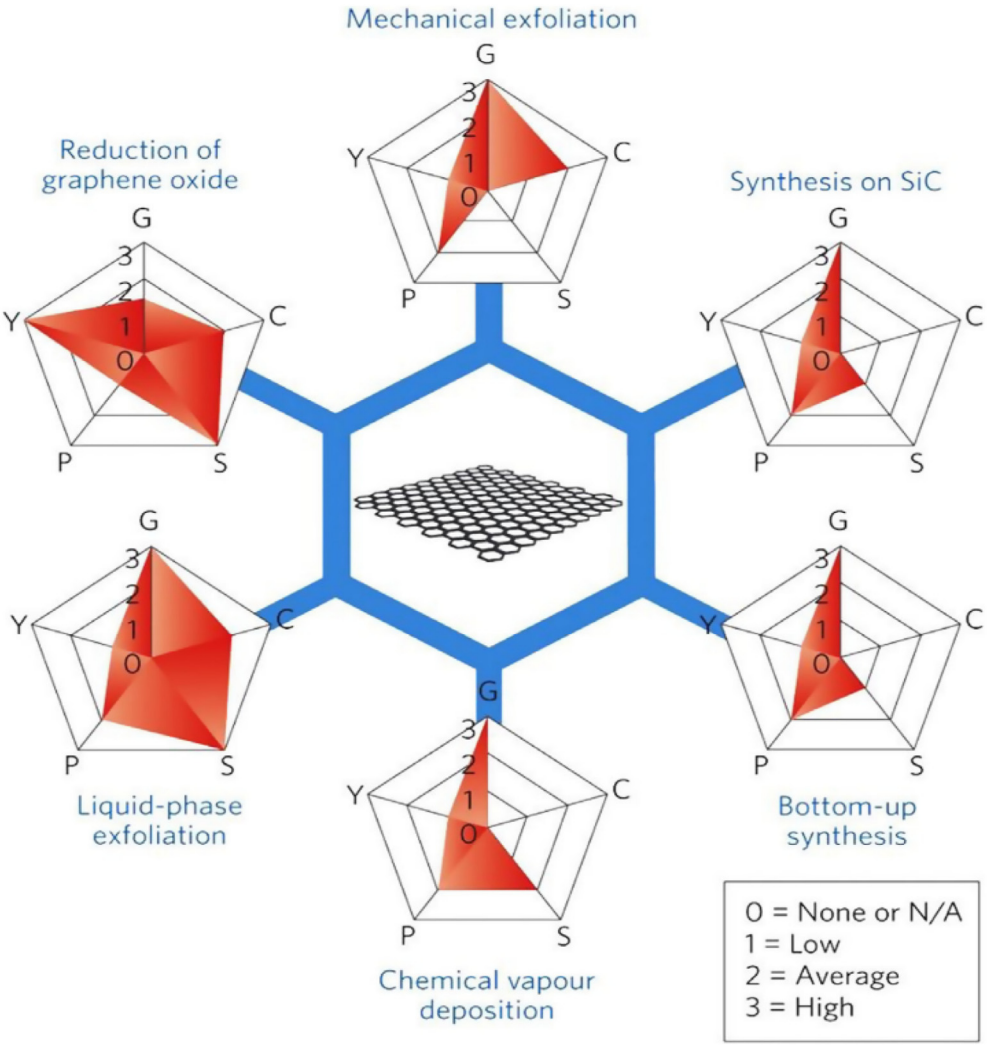

Fig. 6. Key characteristics of the most common graphene production methods in a scale of 0–3: G refers to the graphene quality, C refers to the cost of production (a low value corresponds to high cost of production), S refers to the scalability, P refers to the purity, and Y refers to the yield of each preparation route. Reproduced with permission from Ref. [120]. Copyright 2015, Nature Publishing Group.

pristine tubes are more conductive than the modified ones, the former cannot well disperse in the matrix and (ii) the modified tubes can relatively well disperse in the matrix to create conducting networks.

According to the data listed in Table 2, the modified MWCNTs provide polymers with enhanced electrical conductivity at low filler fractions such as 0.5 wt%. However, considering the cost of modification, in particular for those involving solvent, we recommend using over 5 wt% of pristine MWCNTs.

3. Graphene and derivatives

Monolayer graphene has an electrical conductivity of ~6000 S/cm, whilst graphene (nano)platelets (GNPs or GnPs; each platelet below 10 nm in thickness) have an electrical conductivity of 1460 S/cm [112,113]. Noteworthy is that the first value was measured on a single graphene sheet, but the second one was measured on a thin film consisting of many GNPs where inter-sheet contact resistance reduces much of the conductivity. Monolayer graphene has Young's modulus over 1 TPa and tensile strength around 130 GPa [114], and GNPs have Young's modulus 0.8–1 TPa and tensile strength around 101 GPa [115]. Although the monolayer graphene has higher electrical conductivity, but in terms of mechanical performance, these two types of fillers have no much difference. More importantly, GNPs would be a cost-effective candidate for mass production and polymer industry [116–119].

3.1. Synthesis of graphene

The key characteristics of the most common graphene production methods are graphically illustrated in Fig. 6. Among all six methods, the mechanical exfoliation, chemical vapour deposition (CVD) and graphene oxide reduction methods are briefly discussed below, as details of these methods are available in Raccichini's review [120].

3.1.1. Mechanical exfoliation

In 2004, Geim and Novoselov proved the existence of graphene – monolayer graphite by using mechanical exfoliation [26]. By using scotch tapes, they peeled off thin layers from highly oriented pyrolytic graphite, and these thin flakes were proved to be either monolayer or few-layered graphene [26]. Graphene obtained by this method is nearly perfect in comparison with the reduced GO, and it has no metal residue in comparison with the graphene synthesized by CVD. However, the low production rate limits its application.

3.1.2. Chemical vapour deposition

Chemical vapour deposition (CVD) is widely used in the semiconductor industry to produce thin films. Somani et al. first prepared monolayer graphene thin films by CVD in 2006, where camphor was used as a precursor on Ni foils to form graphene [121]. Since then, CVD has been increasingly employed for large-scale fabrication of graphene films. In general, there are three common approaches: thermal CVD, plasma-enhanced CVD and thermal decomposition [122]. The advantage of each method is briefly summarized below.

The thermal CVD procedure aims to precipitate monolayer carbon from a metal substrate (nickel in most cases) which contains dissolved carbon [123,124]. The thickness and crystalline arrangement of the graphene film can be controlled by cooling rate and carbon concentration. Due to its high efficiency and stability, this method is usually used as a benchmark for comparison with others.

The plasma-enhanced CVD has the advantages of shorter deposition time (below 5 min) and lower operation temperature (650 °C versus 1000 °C for the thermal CVD) [123,124]. The plasma electric field determines the graphene growth direction, and thus it can control the thickness of a graphene film. There are three main parts in the experimental setup of plasma-enhanced CVD, including gas, a plasma generator and a vacuum heating chamber.

In the thermal deposition method, graphene is grown directly by annealing a SiC substrate under ultrahigh vacuum at 1200 °C, where silicon atoms sublimate and leave carbon atoms to self-assemble into honeycomb lattice [123–125]. The annealing time and temperature determine the thickness. This method is the most attractive to the semiconductor industry, because no transfer is required thus retaining high structure integrity. Nevertheless, this method is associated with high operating temperature and costs.

In conclusion, the thermal CVD method is the most efficient to prepare graphene of large lateral dimension. In comparison with the mechanical exfoliation, CVD can produce larger graphene thin films and needs less preparation time. Graphene fabricated via all CVD methods is advantageous of high structure integrity over rGO. Nevertheless, there are challenges yet to be solved, including removal of metal impurity and prevention of graphene winkles on thin films.

3.1.3. Graphene oxide and reduced graphene oxide

Graphene oxide (GO) is a single layer of graphite oxide which was first made by adding graphite into a mixture of potassium chlorate and fuming nitric acid in 1859. In 1898 Staudenmaier et al. improved this work by combining concentrated sulphuric acid with fuming nitric acid and adding potassium chlorate step by step.

Hummers et al. in 1958 summarized previous work and reported the most commonly used method: utilizing $KMnO_4$ and $NaNO_3$ together with concentrated H_2SO_4 to oxidize graphite [126,127]. Graphite oxide shows light brown colour and can attain complete exfoliation and fairly uniform, stable dispersion in water and some organic solvents, due to the

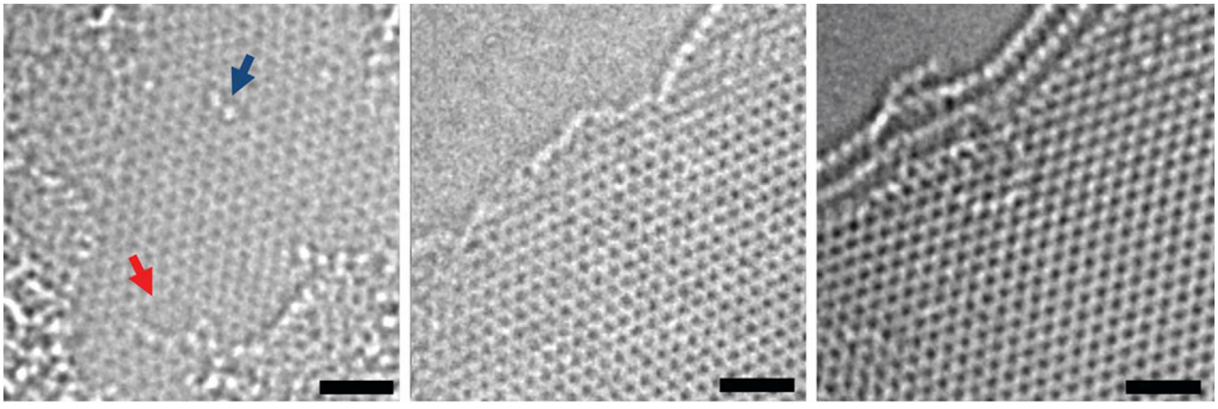

Fig. 7. High-resolution transmission electron microscopy (HR-TEM) micrographs of microwave-reduced GO nanosheets. (a) single-layer chemical reduced GO presenting high density of defects. The red arrow denotes a hole; the blue arrow indicates an oxygen functional group. Bilayer (b) and trilayer (c) MW-rGO showing highly ordered structure. Scale bars, 1 nm, reprinted with permission from Ref. [131], copyright 2016 science group.

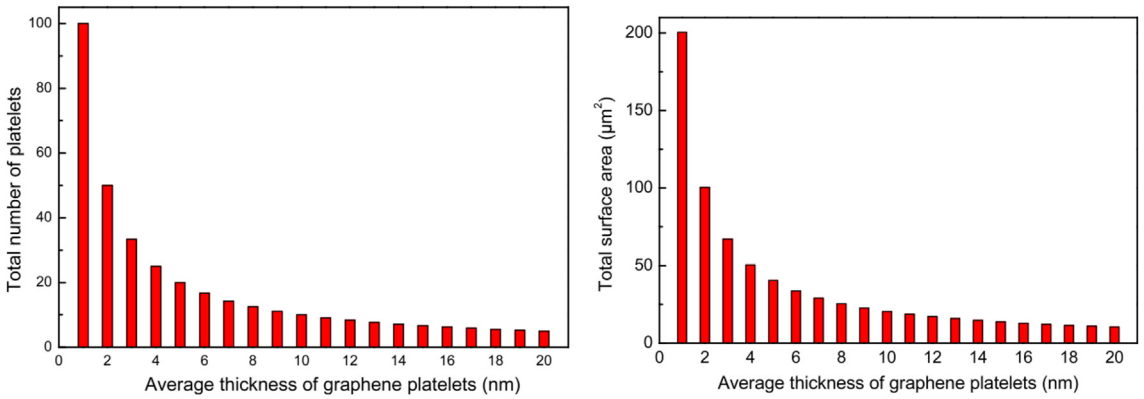

Fig. 8. Number of GNPs (left) and their total surface area (right) in a given volume of a matrix, reprinted with permission from Ref. [50], copyright 2014 Elsevier.

presence of epoxide, hydroxyl and carboxylic groups on graphene sheets. Those functional groups make GO hydrophilic in comparison with pristine graphene. However, these groups also make GO electrically insulating due to the presence of numerous defects which disrupt the sp^2 network [128,129]. Although GO is favoured in the laboratory development of electrode materials, it may not suit polymer composite/processing industry because of relatively high cost as well as low or no electrical conductivity.

To restore graphitic properties, GO is often reduced to graphene-like sheets through chemical means. Protic solvents (e.g. water or alcohol) are used to disperse GO by using sonication or stirring to produce a stable colloid which is then reacted with chemicals such as hydrazine, hydroquinone, UV-irradiated TiO_2, etc., resulting in chemically reduced GO (rGO). The add-on cost of chemicals and toxic emissions likely make this chemical reduction method less favoured in polymer processing and composite industries. As a result, thermal and microwave reduction methods were developed afterwards.

By heating GO at 1000 °C within inert gas for 30 s, the thermal reduction method is able to remove those hydroxyl and carboxyl groups on GO surface. GO in this process can be expanded by hundreds of times and turned into highly winkled rGO [130]. This method does not require extra chemicals, but the resulting wrinkled structures can severely damage the structural integrity of graphene sheets, leading to lower mechanical properties than those obtained from the chemical reduction method.

Using microwave irradiation is an alternative for thermal reduction which reduces operation cost. In a typical process, GO was exposed under a microwave energy of 1000 W for 1–2 S to remove the oxygen-containing groups [131]. The microwave-reduced GO has highly ordered structure in comparison with chemical reduced GO as shown in Fig. 7. However, in comparison with thermal reduction, the microwave radiation is less efficient in mass production due to the limitation of device output. Nevertheless, the comparison should be verified by the data of electrical conductivity, as TEM is limited to localized characterization.

3.2. Graphene nanoplatelets

Graphene (nano)platelets (GNPs or GnPs, few-layer graphene) each have a thickness of below 10 nm. Having far lower preparation costs than monolayer graphene, GNPs contain only 7 wt% oxygen and have exceptional mechanical performance (Young's modulus 0.8–1 TPa, tensile strength around 101 GPa) and high electrical conductivity and thermal conductivity, i.e. 1450 S/cm and 1500–5000 W/m·K [132,133].

GNPs can be synthesized via various methods, such as chemical reduction of slightly oxidized graphite and thermal or microwave expansion of graphite intercalation compounds (GICs). GICs have chemically reactive molecules intercalated between the layers (stages). Upon heating, the intercalated chemicals dramatically vaporized and expanded a GIC into a worm-like product consisting of loosely stacked graphene layers [115].

The number of layers in each graphene nanoplatelet is critical to the physical and mechanical properties of the resulting polymer nanocomposites. The model developed by our team [50] illustrates the effect of platelet thickness on the number of platelets and their total surface area in a given volume of a matrix.

The total number of GNPs (N) in a given volume of a composite is Eq 22 and 23:

$$N = V/v \tag{22}$$

$$v = l \times w \times t \tag{23}$$

where V and v are the nanocomposite and GNPs volumes, respectively, while l, w and t are the length, width and thickness of each graphene nanoplatelet, respectively. Assuming that the volume percentage of GNPs in the nanocomposite is φ%, thus N can be updated as Eq 24:

$$N = (\varphi \times V)/(100 \times l \times w \times t) \tag{24}$$

The total surface area of GNPs (S) inside the nanocomposite can be computed as Eq 25

$$S = (2 \times l \times t + 2 \times l \times w + 2 \times w \times t) \times N \tag{25}$$

Assuming that: (i) the volume of the nanocomposite is 10 μm^3, (ii) GNPs are at a percentage of 1 vol%, (iii) each platelet is a rectangular cuboid of 1 × 1 μm, the total number of GNPs equals Eq 26:

$$N = \frac{\left(10 \times 10^9\ (nm^3)\right) \times 1}{100 \times 1 \times 1000\ (nm) \times 1 \times 1000\ (nm) \times t\ (nm)} \tag{26}$$

The total surface area of GNPs is Eq 27:

$$S = (2 \times 1 \times 1000 \times 1 \times 1000 + 4 \times 1000 \times t) \times N \tag{27}$$

In Fig. 8, both the GNP number and the total surface area reduce dramatically when the thickness increases from 1 to 10 nm, demonstrating the necessity to keep the thickness as low as possible. It is also essential to delaminate these nanoplatelets in polymers.

As the expanded product was reported for low specific surface area [134], it was treated in organic solvent such as acetone by ultrasonication, to produce GNPs. Their thickness was measured as 2–5 nm [133], and so each platelet should consist of 2–5 layers of graphene due to wrinking. However, monolayer graphene might exist when GNPs are dispersed in epoxy. *N*-methyl-2-pyrrolidone (NMP) was reported as the best solvent to create GNPs through 30–60 min of ultrasonication below 30 °C [135]. The controlled, relatively low temperature is essential during the sonication [115]. As illustrated in Fig. 9, after thermal expansion, long-chain amine-end molecules can be grafted onto the GNP surface, to significantly improve the exfoliation and dispersion of GNPs in epoxy.

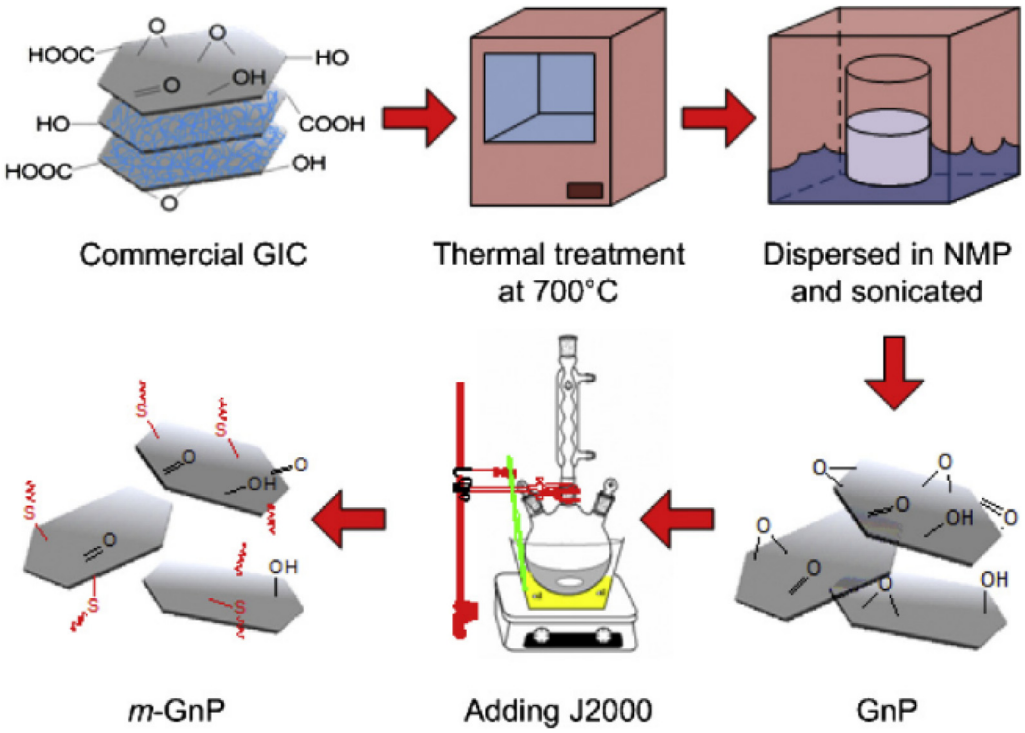

Fig. 9. Schematic of covalent modification of graphene nanoplatelets, reprinted with permission from Ref. [135], copyright 2014 Elsevier.

Microwave radiation can also be used to produce GNPs. Naeem et al. reported a facile, green and novel approach to preparation of epoxy/graphene nanocomposites [136]. The approach involves microwaving a commercial graphene precursor and mechanically stirring to produce GNPs in hot epoxy, without the need for organic solvents and external surfactants. Containing single-layer graphene, the resultant GNPs are 4.17 ± 0.63 nm in thickness and 1.00–4.77 μm in lateral dimension. The platelets provided epoxy with remarkable improvements of mechanical and functional properties, e.g. a 175% increment of critical strain energy release rate at 1.03 vol% of graphene, a 14.9% increment of Young's modulus at 1.55 vol%, and a percolation threshold of electrical conductivity at 0.85 vol%. As the measurement of fracture toughness is highly sensitive to crack sharpness [137], an instantly propagated crack was introduced to each compact tension specimen. The glass transition temperature of epoxy was enhanced from 85.4 to 100.0 °C at 1.03 vol%.

Although the mechanical performance of GNPs is slightly lower than monolayer graphene [138], GNPs are much cheaper. Based on the quotation from Asbury Carbons, the price of GICs is at US$ 4 per kg, depending on the quantity quoted. After expansion and ultrasonication, the total cost of GNPs was estimated to be US$ 10–20 per kg [133]. This makes GNPs more favourable as a class of nanofillers than monolayer graphene for polymer composite and processing industries. In 2018, our team extensively reviewed the fabrication and application of GNPs [138].

3.3. Polymer/graphene nanocomposites

Superior to MWCNTs, graphene (nano)platelets (GNPs or GnPs; each platelet below 10 nm in thickness) feature extraordinary specific surface area. By grafting functional groups on their surface, the relatively inert surface of GNPs can be fundamentally changed, thus improving their dispersion in and enhancing interactions with the polymeric matrices. With a sufficient number of platelets relatively uniformly dispersed in polymer matrices, continuous networks were created for low percolation thresholds of electrical conductivity in many cases [139,140]. This section will examine the influence of GNPs and the composite preparation methods.

3.3.1. Mechanical properties

The effect of GNP surface modification on thermoset polymers is discussed below. The modified GNPs are well known for improving the stiffness and fracture toughness of epoxy, because GNPs were modified

Table 3
Mechanical properties of polymer/GNP nanocomposites.

Matrix	Filler Type	Filler Fraction (wt %)	Young's Modulus (GPa); polymers	Tensile Strength (MPa); polymers	Young's Modulus (GPa) and increment %; composites	Tensile Strength (MPa) and increment %; composites	Ref.
SBR	Pristine GNPs	5	0.89	2.16	1.31 (47.2%)	5.86 (171.3%)	[144]
Nylon 66	Pristine GNPs	0.3	0.92	55.17	0.83 (-9.8%)	63.56 (15.2%)	[150]
PVA	Reduced GO	0.1	1.74	65.7	2.69 (54.6%)	75.0 (14.2%)	[146]
PMMA	Modified GNPs	2	1.05	13	1.25 (19.0%)	22(69.2%)	[151]
HDPE	Pristine GNPs	1	N/A	22	N/A	23 (4.5%)	[152]
PC	Pristine GNPs	7	2.45	58.0	3.65 (49.0%)	62.5 (7.8%)	[153]
PS	Reduced GO	0.1	1.80	48	2.29 (27%)	50 (4.2%)	[154]

Table 4
Electrical conductivity of GNPs-containing nanocomposites.

Matrix	Filler type	Filler fraction (vol%)	Fabrication approach	Conductivity ($S{\cdot}cm^{-1}$)	Ref.
Epoxy	Pristine GNPs	0.8	*In-situ* polymerization	5.1×10^{-4}	[155]
Epoxy	Modified GNPs	0.8	*In-situ* polymerization	1.4×10^{-3}	[155]
Epoxy	Pristine GNPs	0.5	*In-situ* polymerization	3.8×10^{-13}	[147]
EPDM	Pristine GNPs	26.7	Melt compounding	4.1×10^{-8}	[50]
HDPE	Modified GO	2.5	*In-situ* polymerization	1.02×10^{-7}	[148]
Nylon 6	Reduced GO	1.66	Melt compounding	5.5×10^{-6}	[149]
PVDF	Pristine GNPs	16.1	Solution blending	5.1×10^{-3}	[156]

either with molecules whose structure was similar to epoxy or with CNTs, thus potentially promoting the exfoliation and dispersion [116,119,133,135,141,142]. Noteworthy is that the chain length of the molecules grafted on nanosheets may pose a remarkable effect on the resulting composites [142] Under loading, the grafted molecules can firmly lock GNPs with host polymer chains to facilitate stress transfer across the interface. The surface modification of GNPs is extensively reviewed by Yu et al. [143].

Apart from the surface modification, the preparation method is important to the morphology and properties of the resulting composites. In Table 3, an increment of 47.2% in Young's modulus was attained for a styrene-butadiene rubber (SBR)/GNP nanocomposite at a filler fraction of 5 wt%, which was prepared by melt compounding [144]. *In-situ* polymerization is often used to prepare elastomer nanocomposites. It is advantageous to preventing GNPs from restacking within the matrix. Introducing functional groups onto the platelet surface can improve the compatibility for the composites, making GNPs a promising candidate for elastomer reinforcement. However, some challenges remain. Elastomers require high molecular weight to attain sufficient elongation, but *in-situ* polymerization may limit the growth of long-chain molecules due to the steric effect posed by nanosheets during fabrication.

Similar to thermoset polymers, both the surface modification and preparation methods are vital for thermoplastic polymers. Maccaferri et al. reported an industry-friendly approach to preparing nylon/GNP composite nanofibers by electrospinning, where an increment of 59% in Young's modulus and 85% in tensile stress were reported at 1.5 wt% [145]. Pristine GNPs were found to pose a remarkable effect on the fibre diameter, and a phenomenological model was used to investigate the GNP contribution. Noteworthy is that the most cost-effective approach – melt compounding – was used to prepare certain nanocomposites listed in Table 3. An extensometer indispensable in tensile testing measures the change of gauge length in the middle region which has a constant cross section area along the sample length. The calculation of Young's modulus must be made by using the slope in the initial straight portion of a stress-strain graph, and the strain range used for the slope must be reported. Statistical analysis should be undertaken for the data. However, these important experimental requirements are often neglected in some studies, causing unexplainable testing results, such as reduction in modulus albeit increase in strength for polymer/graphene nanocomposites.

From our perspective, surface modification of GNPs could further enhance these improvements but the modification must be conducted in a way acceptable to thermoplastic processing industry. It is worth noting that chemical modification usually causes irreversible damage to the graphitic structure of GNPs. Thus, a non-covalent approach was proposed by Wang et al. who wrapped the rGO surface with poly (sodium 4-styrenesulfonate). This method prevents the agglomeration of rGO in a PVA matrix without causing damage to the filler structure [146]. A 54.6% increase in Young's modulus was made at 0.1 wt% and 14.2% in tensile strength were obtained at 0.1 wt%, due to the strong physical molecular interactions between PVA and rGO.

3.3.2. *Electrical properties*

Table 4 reveals the effect of GNPs and GO on the conductivity of different polymer matrices. For thermoset polymers such as epoxy and SBR, the filler surface modification poses an obvious effect on the conductivity of final composites at low fractions. An epoxy/modified GNP nanocomposite at 0.5 vol% displays higher conductivity than neat epoxy, i.e. 3.8×10^{-13} $S{\cdot}cm^{-1}$ vs 3.39×10^{-16} $S{\cdot}cm^{-1}$ [147]. This is because the surface modification significantly improves the filler dispersion and promotes the formation of conductive network. Although the modified GNPs have lower electrical conductivity, the resulting nanocomposite has a higher electrical conductivity due to relatively uniform dispersion than the unmodified one. However, it is not clear whether surface modification is still highly effective to thermoset polymers containing high fractions of GNPs.

For thermoplastics, both surface modification and composite preparation are essential. In 2018, Cruz-Aguilar et al. investigated the effect of graphene oxidation on the HDPE conductivity. An HDPE/highly oxidized graphene nanocomposite at 1.0 wt% and 5.8 wt% shows conductivity of 9.09×10^{-10} $S{\cdot}cm^{-1}$ and 1.02×10^{-7} $S{\cdot}cm^{-1}$ respectively [148]. We conclude that the resulting nanocomposite conductivity should directly relate to the oxidization level of conductive fillers and that it is vital to strike a delicate balance between the filler dispersion and conductivity. It is worth noting that nylon/rGO nanocomposites fabricated by melt compounding exhibited antistatic performance. The electrical conductivity of the nanocomposites increases with filler fractions, with a conductive network of rGO observed at 1.66 vol% [149]. The comparison

Table 5
Comparison of mechanical properties for polymer nanocomposites.

Matrix	Filler Type	Filler Fraction (wt %)	Young's Modulus (GPa); polymers	Tensile Strength (MPa); polymers	Young's modulus (GPa) and increment %; composites	Tensile strength (MPa) and increment %; composites	Ref.
Epoxy	Pristine GNPs	3.0	1.48	46.46	1.64 (10.8%)	49.78 (7.1%)	[157]
Epoxy	Pristine MWCNTs	3.0	1.48	46.46	1.69 (14.2%)	54.48 (17.3%)	[157]
PVA	Modified MWCNTs	0.5	0.0166	19.11	0.0329 (98.2%)	34.60 (81.1%)	[158]
PVA	Graphene oxide	0.3	2.32	25.3	5.82 (150.9%)	63.0 (149.0%)	[159]
PES	Pristine MWCNTs	1.0	0.045	1.70	0.067 (48.9%)	2.38 (40.0%)	[160]
PES	Graphene oxide	1.0	1.16	30.79	1.95 (68.1%)	55.73 (81.0%)	[161]
HDPE	Modified MWCNTs	2.5	0.75	26.5	1.15 (53.3%)	34.5 (30.2%)	[105]
HDPE	Prinstine GNPs	10	0.96	27.2	1.49 (55.2%)	33.4 (22.8%)	[162]

reveals that the nanofillers have potential to replace conventional micron-sized antistatic agents (such as stainless-steel fibres) in the thermoplastic processing industry.

In conclusion, according to the data listed in Table 4, the surface modification of GNPs and GO is indispensable in most cases, since it can significantly improve the filler dispersion and thus enhance the resulting nanocomposites' conductivity. However, over-modified filler surface damages the structure integrity of the fillers and severely reduces their conductivity, which would subsequently reduce the conductivity of the resulting nanocomposites. Hence, a balance is needed between the structure integrity and the quantity of defects for surface modification. On the other hand, fabrication methods significantly influence the dispersion of GNPs and GO in polymers and determine the performance of the resulting nanocomposites. Therefore, extensive investigation is needed to cost-effectively disperse GNPs in polymers, to pave a way for the scaleup production of these polymer nanocomposites.

4. Comparison of nanocomposites containing MWCNTs and graphene

4.1. Mechanical properties

Although graphene (nano)platelets (GNPs or GnPs; each below 10 nm in thickness) can be dispersed in polymers effectively by simple mixing, the filler reinforcing effect in many cases may not be as effective as MWCNTs. As listed in Table 5, an epoxy/MWCNT nanocomposite at 3 wt % was reported to have an increment of 17.3% in tensile strength and 14.2% in Young's modulus over neat epoxy [157]. However, an epoxy/GNP nanocomposite at the same filler loading demonstrated less improvements – 7.1% and 10.8%. This is because the cylindrical structure of MWCNTs has more interactions with the matrix through both large tube surface and mechanical interlocking with polymer chains.

Graphene oxide (GO) has been proved advantageous for compounding with hydrophilic polymers. By functionalizing the surface of MWCNTs with PVA, Yadav et al. found that MWCNTs at 0.5 wt% improved the tensile strength and Young's modulus of neat PVA by 81.1% and 98.2%, respectively [158]. In contrast, Kashyap et al. reported that GO at 0.3 wt% significantly increased the tensile strength and Young's modulus of neat PVA by 149.0% and 150.9% [159], which was contributed by the hydrophilic nature and high surface roughness and specific surface area of GO.

GNPs showed promise in forming composites with poly (ether sulfone) (PES). A PES/MWCNT nanocomposite at 1.0 wt% demonstrated an increment of 40.0% in tensile strength and 48.9% in Young's modulus [160]. However, a PES/GO nanocomposite at 1 wt% revealed an 81.0% increment in tensile strength and a 68.1% increment in Young's modulus [161]. From our perspectives, the lower performance of PES/MWCNT nanocomposite is probably caused by the entanglement of MWNCTs in the matrix. More research is clearly needed as the reported modulous of neat PES is substantially lower than the literatrue.

Lin et al. prepared nanocomposites by an environmentally friendly approach – melt compounding where no solvent was needed. The tensile strength and Young's modulus of a HDPE/GNP nanocomposite at 10 wt% were improved by 22.8% and 55.2% [162], whereas at 2.5 wt% the HDPE/MWCNT nanocomposite demonstrated 30.2% and 53.3% improvements in tensile strength and Young's modulus [105]. This may indicate that the melt compounding method is not highly effective in disentangling and dispersing MWCNTs in HDPE.

To conclude, both MWCNTs and GNPs can improve the mechanical properties of most polymers. MWCNTs are able to enhance the mechanical properties more effectively as long as they are relatively uniformly dispersed in thermoset matrices such as epoxy via *in-situ* polymerization. GNPs should be preferred if they can be directly exfoliated in thermoplastic matrices such as polycarbonate via melt compounding. This is likely because (i) at high fractions GNPs are less susceptible to agglomeration than MWCNTs and (ii) the layered structure can readily form oriented percolation networks to transport kinetic energy. Utilizing both MWCNTs and GNPs may create an obvious synergy for polymers, as to be discussed in the following sections.

Table 6
Comparison of electrical conductivity for polymer nanocomposites.

Matrix	Filler type	Filler fraction (wt%)	Preparation method	Conductivity ($S{\cdot}cm^{-1}$)	Ref.
Epoxy	Pristine MWCNTs	1.5	*In-situ* polymerization	1.0×10^{-5}	[167]
Epoxy	Pristine GNPs	1.2	*In-situ* polymerization	1.0×10^{-4}	[167]
PES	Modified MWCNTs	20	Solution mixing	4.5	[165]
PES	Reduced GO	~ 0.2	Solution mixing	9.6×10^{-6}	[164]
PS	Pristine MWCNTs	10.0	Melt compounding	1.3	[166]
PS	Pristine GNPs	10.0	Melt compounding	7.07	[166]
PANI	Modified MWCNTs	5.5	*In-situ* polymerization	1.6×10^{-1}	[168]
PVC	Pristine MWCNTs	0.5	Solution/melt mixing	1.0×10^{-7}	[169]
PVC	Ball milled graphene	1.0	Melt compounding	4×10^{-7}	[170]

4.2. Electrical properties

The electrical conductivity of nanocomposites depends on the properties of the matrix, the properties and dispersion of the filler, and their interface. The filler dispersion is critical to the electrical conductivity of the resulting nanocomposites, because nanofillers usually aggregate, agglomerate or form clusters due to their high specific surface area. The formation of a conductive network is a prerequisite for anti-static or electrically conductive nanocomposites. Table 6 compares the electrical conductivities of a number of polymer nanocomposites respectively containing either MWCNTs or GNPs.

As reported by Ivanov et al., the exceptional aspect ratio of MWCNTs greatly promoted the electrical conductivity of PLA. A PLA/MWNCT nanocomposite at 6 wt% exhibited a conductivity of $2.1 \times 10^{-4}\ S{\cdot}cm^{-1}$, in comparison with $8.4 \times 10^{-5}\ S{\cdot}cm^{-1}$ for a benchmark PLA/GNP nanocomposite [163]. This is likely because the melt extrusion method was effective in disentangling MWCNTs but not in exfoliating those stacked GNPs sheets.

The electrical conductivity of a PES/rGO nanocomposite at about 0.2 wt% was found to be $9.6 \times 10^{-6}\ S{\cdot}cm^{-1}$ [164], much lower than that of the PES/MWCNT nanocomposite, $4.5\ S{\cdot}cm^{-1}$ at 20 wt% [165], likely due to the low conductivity of rGO. A different conclusion was found for PS nanocomposites. An electrical conductivity of $7.07\ S{\cdot}cm^{-1}$ was reported for a PS/GNP nanocomposite at 10 wt%, but it was dropped to $1.3\ S{\cdot}cm^{-1}$ for a PS/MWCNT nanocomposite [166]. These extraordinary conductivity values need to be reproduced by other groups. The result was explained as MWCNTs at high fracitons can more readily aggregate during the melt compounding procedure than GNPs.

The remaining Table 6 includes the conductivity values of the nanocomposites based on polyaniline (PANI) and polyvinyl chloride (PVC). In comparison with GNPs, MWCNTs have shown overall better performance at low filler fractions (<10 wt%); MWCNTs may have obtained relatively uniform dispersion within polymer matrices, forming an effective conductive network. At higher fractions, MWCNTs can readily reaggregate. Due to relatively low lateral dimension, GNPs are less efficient at low fractions than MWCNTs. But at high fractions GNPs are less susceptible to agglomerate, which may lead to higher performance in improving electrical conductivity than MWCNTs. Many more studies are needed to compare MWCNTs with GNPs regarding their dispersion in

Table 7
Properties and synergy rates of polymer/MWCNT/graphene nanocomposites.

Matrix	MWCNT: graphene mixing ratio	Filler fraction (wt %)	Preparation method	Young's modulus (GPa) Synergy rate	Tensile strength (MPa) Synergy rate	Conductivity ($S \cdot cm^{-1}$)	Ref
PP	1:1	1	Melt compounding	1.82 (10.6%)	40 (14.3%)	6.3×10^{-10}	[174]
PMMA	1:2	3	Supercritical fluid Assisted processing	2.85 (2.7%)	63.0 (20.0%)	2×10^{-9}	[180]
PMMA	1:1	3	Supercritical fluid Assisted processing	3.00 (8.1%)	60.0 (14.3%)	3×10^{-8}	[180]
PMMA	2:1	3	Supercritical fluid Assisted processing	2.80 (0.9%)	56.5 (7.6%)	1×10^{-7}	[180]
Epoxy	1:1	0.5	Mechanical blending	3.1 (33.6%)	66.2 (21.4%)	N/A	[177]
Epoxy	4:1	0.8	Mechanical blending	N/A	N/A	6×10^{-8}	[181]
Epoxy	1:4	0.8	Mechanical blending	N/A	N/A	8×10^{-14}	[181]

matrices and the mechanical and functional properties of the resulting nanocomposites.

5. Synergistic effects in polymer/MWCNT/graphene nanocomposites

A synergistic effect is generally defined as a hybrid improvement which cannot be achieved by each phase working alone. Many studies have proven that such an effect does exist in composites containing micron-fillers. MWCNTs and graphene nanoplatelets (GNPs; each platelet below 10 nm in thickness) have recently shown significant synergistic effects on enhancing the properties of polymer nanocomposites [171–173]. Ping et al. evaluated the synergy of MWCNTs and rGO for polypropylene (PP) by the following equation Eq 28 [174]:

$$Synergy\ (\%) = \frac{2P_{CG} - (P_C + P_G)}{P_C + P_G} \times 100 \tag{28}$$

where P_{CG}, P_C and P_G represent the mechanical properties of three nanocomposites: PP/MWCNT/rGO, PP/MWCNT and PP/rGO.

In Table 7, a PP/MWCNT/rGO nanocomposite at a hybrid filler ratio of 1 exhibits synergy rates of 14.3% and 10.6% for tensile strength and Young's modulus, respectively. When NBR was utilized as a host matrix to compound with different ratios of MWCNTs to GNPs [175], synergy rates of 56% and 52% were observed for tensile strength and Young's modulus respectively at a mixing ratio of 1:3. Similar results were confirmed by Chatterjee et al. who proved that MWCNTs usually play a major role in an epoxy/MWCNT/GNP nanocomposite [176]. By increasing the MWCNTs to GNPs ratio, MWCNTs should have more opportunities to work as the bridges connecting and kniting GNPs into conductive junctions within polymer matrices. At the same time, GNPs work as the seperators to prevent MWCNTs from entangling with each other during preparation. Although the hybrids have displayed significant synergistic effects, appropriate molecular interactions between MWCNTs and GNPs upon surface modification may lead to higher performance from our perspectives. Noteworthy is that the polymer structure can significantly affect the synergistic effect of hybrid fillers. It is important to choose an appropriate hybrid filler ratio for different polymers.

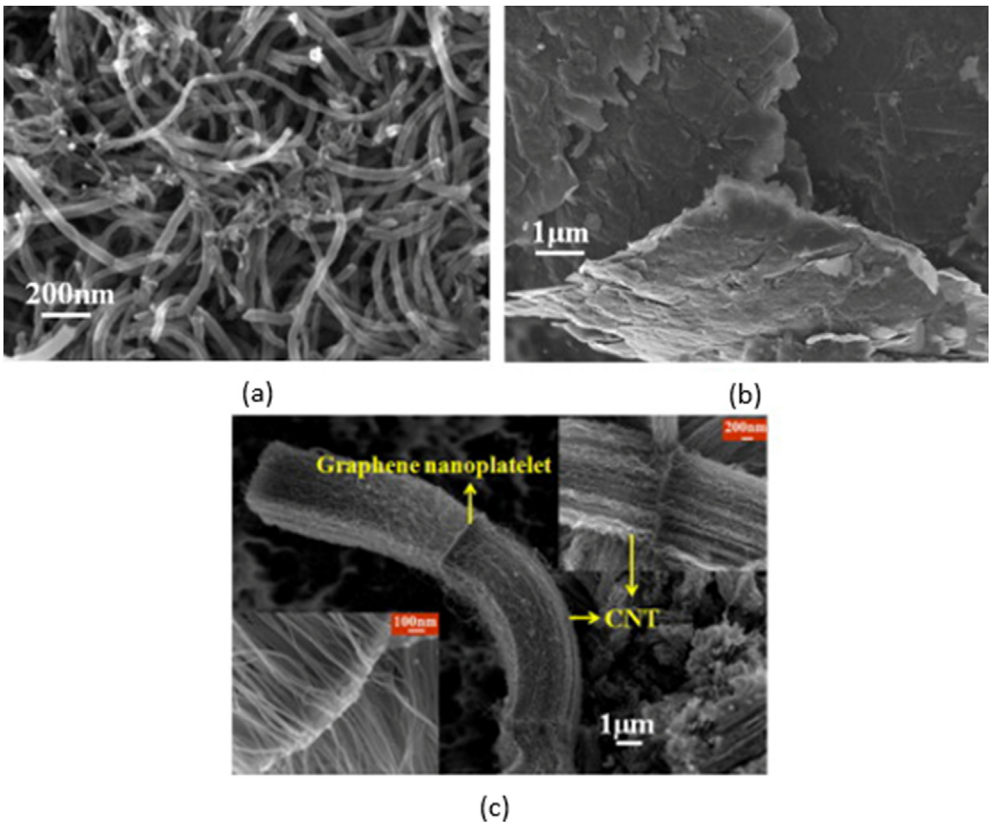

Fig. 10. SEM micrographs of (a) MWCNTs, (b) GNPs and (c) MWCNT–GNP hybrids, reprinted with permission from Ref. [177], copyright 2013 Elsevier.

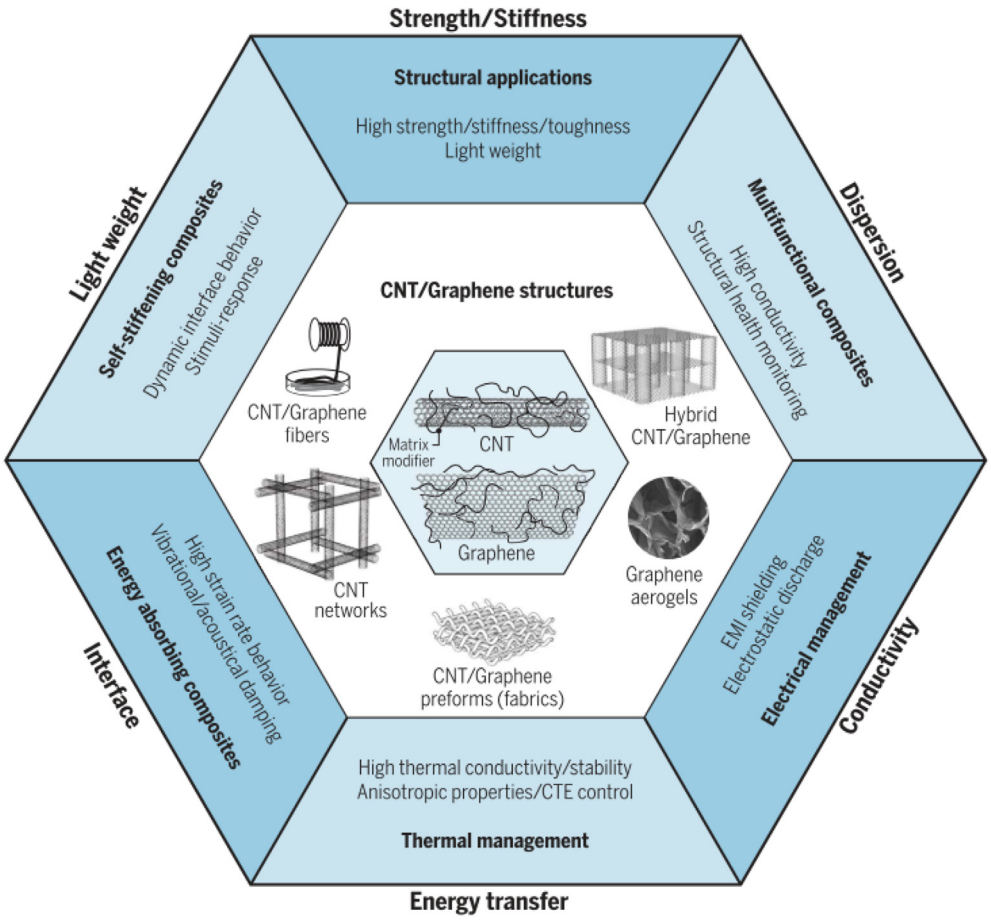

Fig. 11. A schematic summarizing various MWCNT and GNP composites with anticipated enhanced properties for the prospective applications along with six key parameters, reprinted with permission from Ref. [54], copyright 2018 Science.

To build bonding between MWCNTs and GNPs, Li et al. reported a chemical vapour deposition (CVD) method to grow MWCNTs on the GNP surface [177]. In Fig. 10, the GNP surface is densely covered with MWCNTs. These hybrid fillers were dispersed in epoxy resin by using a three-roll mill. As a result, the 0.5 wt% nanocomposite showed a 21.4% synergy rate for tensile modulus and 33.6% for Young's modulus at a hybrid filler mixing ratio of 1. Noteworthy is that syngas production was used for one-pot synthesis of CNT/graphene hybrids [141], although these have not yet been compounded with any polymer. From our perspectives, the dispersion and interaction of these hybrid fillers in a matrix could be improved with surface modification.

The synergistic effect not only enhances the mechanical and electrical properties of polymer nanocomposites, but also improves the thermomechanical properties and electromagnetic shielding ability. As reported by Manoj et al., both GNPs and MWCNTs upon surface modification were mixed at ratios (1:1, 1:3 and 3:1), and then the hybrid fillers were added into epoxy via solution mixing. By thermogravimetric analysis, a maximum gain of 20% was reported for the sample with a filler ratio of 3:1 in comparison with solo filler nanocomposites [178], which proved that the synergistic effort can significantly boost the thermomechanical properties of thermoset polymers such as epoxy.

On the other hand, Meenakshi et al. fixed the mixing ratio of GNPs to MWCNTs at 1, and utilized solution mixing to prepare polyurethane nanocomposites for electromagnetic shielding [179]. A nanocomposite at 10 wt% exhibited excellent electromagnetic interference shielding up to −47 dB.

These research outcomes have proved the significance of synergy for hybrid fillers in polymer nanocomposites. However, more comprehensive and extensive studies are needed to address the following questions: Whether surface modification is vital for both fillers? What is the influence of polymer structure on the dispersion of hybrid fillers? And how to reduce the cost of hybrid fillers for industry?

6. Prospect and challenges of carbon-based nanofillers for polymers

The size and geometry of MWCNTs and graphene (nano)platelets (GNPs or GnPs; each platelet below 10 nm in thickness) make them ideal in reinforcing or toughening polymers and providing them with new functionalities. Due to zero toxicity rating in CHEMWATCH, GNPs hold promise for polymer processing and composite industries. Based on our communications with Shandong Dazhan Nano Materials CO. and Asbury Carbons™, the market prices for MWCNTs and GNPs are approximately US$ 30 and potentially US$ 10–20 per kg. High performance and reasonable costs make these carbon nanofillers competitive. Nevertheless, the following challenges need to be addressed.

(i) *Disentanglement and modification of MWCNTs.* Harsh conditions such as long-time milling, sonication and chemical oxidization often break MWCNTs into short rods, severely reducing the bridging effects of MWCNTs within matrices. Investigation is needed to strike a balance between surface modification and fragmentation.

(ii) *Reaggregation.* Melt compounding is preferred in thermoplastic processing industry, but the reaggregation/entanglement of MWCNTs constantly occurs, compromising the composites' properties especially at low filler fractions. Filler surface modification works for thermoplastic/MWCNT nanocomposites to some

degree, but it is not highly effective for thermoset polymers such as epoxy resins, as reaggregation often occurs during curing.

(iii) *Interface.* The interface between MWCNTs and polymeric matrices determines the dispersion of MWCNTs and their interactions with polymers, dominating the resulting nanocomposite properties. Three issues are described below:
- How to produce a sufficient number of reactive sites on the MWCNTs' side walls without causing much damage to the filler?
- The organic molecules grafted on MWCNTs have three ways to interact with matrix molecules, i.e. covalently bonding, molecular entanglement and π–π interaction; of these, it is not clear which one is the strongest, whether a strong interface is really needed, and what is the effect of interfacial strength on the nanocomposites' properties.
- Instead of interacting with host polymer matrices, the grafted molecules might interact with each other and cause severe reaggregation of MWCNTs. Thus, the surface modification must be carefully designed, conducted and examined.

Weaving MWCNTs into micron size fibres is a relatively new research direction. MWCNT fibres and fabrics in future may by sufficiently cost-effective to replace conventional fillers for electrostatic discharge applications.

On the other hand, graphene nanoplatelets (GNPs) are favoured due to potential cost-effectiveness, and their average thickness is determined by the oxidation and intercalation process of graphite as well as the subsequent expansion/exfoliation conditions. When GNPs are mixed with a polymer, platelets may either stack themselves, aggregate or form clusters even though they may readily exfoliate in another polymer matrix; once stacked, GNPs may perform similarly to graphite which is known for lubrication. This challenge must be addressed altogether with the following issues.

(i) *Lateral dimension and thickness control.* GNPs with low thickness could lead to better mechanical properties and electrical/thermal conductivity for the resulting polymer nanocomposites. However, the oxidization and exfoliation procedures often reduce the lateral dimension.

(ii) *Control of surface modification.* Thermal shock or microwave expansion followed with ultrasonication is the most common way to prepare GNPs. The number and locations of epoxide groups produced during the preparation are vital to the interface strength and thus the resulting nanocomposite properties. It is not clear whether the atmospheric conditions pose a detrimental impact on the number and locations. New inexpensive methods are needed to produce GNPs having a tuneable quantity of surface functional groups.

(iii) *Thermal conductivity control.* The thermal conductivity of polymer nanocomposites may not increase linearly with GNPs as theory predicted [182], to which interface modification causes uncertainty. Thermal transfer relates to phonon energy movement which is limited by filler–filler and filler–polymer interfaces. It requires further studies to establish the relationship between thermal conductivity and interface modification.

(iv) *Solvent*-free synthesis of polymer/graphene nanocomposites. Green, facile preparation methods are urgently needed, since solvent is not tolerated in most polymer processing and composite industrial sectors. Within this context, our team reported a graphene precursor which in epoxy at 200 °C is able to directly exfoliate into three classes of GNPs: (i) large, single-layer graphene, (ii) medium sized sheets with 5.2 ± 1.95 nm in thickness and (iii) smaller 0.5–1.0 nm thick sheets of 200–500 nm in lateral dimension, with a Raman I_D/I_G ratio of 0.177. Platelet films of ~10 μm in thickness have an electrical conductivity of 978.65 ± 79.44 S/cm. A percolation threshold of electrical conductivity is observed at 0.80 vol% for epoxy/GNP nanocomposites. At 1.03 vol%, the nanocomposite has a fracture energy release rate of 850.78 ± 58.00 J m^{-2} corresponding to an increase of 170.6% over neat epoxy [147].

Recent progress of synthesizing various hybrids of MWCNTs and GNPs would provide an opportunity to translate their exceptional properties into a variety of engineering applications. MWCNTs are able to bridge individual platelets and provide efficient transfer routes for stress, electrons and phonons. Thus polymer/GNP/MWCNT nanocomposites demonstrate higher performance in comparison with two-phase nanocomposites: i.e. polymer/MWCNT and polymer/GNP. The mixing ratio of MWCNTs to GNPs determines the synergy rate, and the interface between filler and matrices may significantly enhance the performance of polymer nanocomposites. The challenges are to identify the best mixing ratio and to investigate the influence of interface modification on the synergy and the various properties of polymer nanocomposites.

It can be envisioned that, if carefully designed and optimized, polymer/MWCNT/GNP nanocomposites should not only provide support to or even replace those polymer/carbon fibre composites but also create new functionalities, such as stimuli-responsiveness, energy storage and conversion elements, real-time structural health monitoring, sensing and vibrational damping in composites. A range of perspective applications, including structural applications, multifunctional nanocomposites, electrical and thermal management, energy-absorbing nanocomposites and self-stiffening nanocomposites with the required properties, are summarized in Fig. 11 along with six key parameters, including strength/stiffness, lightweight, interface, energy transfer, conductivity and dispersion in the nanocomposite design and manufacturing.

7. Conclusion

MWCNTs and graphene (nano)platelets (GNPs or GnPs; each platelet below 10 nm in thickness) are proper candidates for the development of polymer nanocomposites. Increasingly more interests are attracted in both academia and industry for cost-effectively combining MWCNTs and GNPs to create synergy for polymers. In comparison with GNPs, MWCNTs in most cases have shown strong reinforcement for polymers at low filler fractions (<10 wt%) where these tubes may remain relatively uniform dispersion and form an effective conductive network. At higher fractions, MWCNTs may readily reaggregate and form large agglomerations. Binding MWCNTs with GNPs at a mixing ratio of 1:1 has shown a significant synergistic effect on reinforcing polymer, in comparison with two-phase nanocomposites. In summary, high structural integrity, reasonable market price and availability for facile surface modifications make MWCNTs and GNPs promising candidates for polymer nanocomposites.

Declaration of competing interest

The authors declare that they have no conflict of interest.

Acknowledgement

The authors thank financial support by the Australian Research Council (LP180100005 & DP200101737).

References

[1] H. Staudinger, Uber polymerization (on polymerization), Ber. Dtsch. Chem. Ges. 53 (1920) 1073–1085, https://doi.org/10.1002/cber.19200530627.
[2] M. Moussa, G. Shi, H. Wu, Z.H. Zhao, N.H. Voelcker, D. Losic, J. Ma, Development of flexible supercapacitors using an inexpensive graphene/PEDOT/MnO2 sponge composite, Mater. Des. 125 (2017) 1–10, https://doi.org/10.1016/j.matdes.2017.03.075.
[3] A. Alam, Y.J. Zhang, H.C. Kuan, S.H. Lee, J. Ma, Polymer composite hydrogels containing carbon nanomaterials-Morphology and mechanical and functional performance, Prog. Polym. Sci. 77 (2018) 1–18, https://doi.org/10.1016/j.progpolymsci.2017.09.001.

[4] M. Moussa, M.F. El-Kady, S. Abdel-Azeim, R.B. Kaner, P. Majewski, J. Ma, Compact, flexible conducting polymer/graphene nanocomposites for supercapacitors of high volumetric energy density, Compos. Sci. Technol. 160 (2018) 50–59, https://doi.org/10.1016/j.compscitech.2018.02.033.
[5] S.W. Lu, J.Y. Shao, K.M. Ma, D. Chen, X.Q. Wang, L. Zhang, Q.S. Meng, J. Ma, Flexible, mechanically resilient carbon nanotube composite films for high-efficiency electromagnetic interference shielding, Carbon 136 (2018) 387–394, https://doi.org/10.1016/j.carbon.2018.04.086.
[6] A.D. Qiu, P.L. Li, Z.K. Yang, Y. Yao, I. Lee, J. Ma, A path beyond metal and silicon: polymer/nanomaterial composites for stretchable strain sensors, Adv. Funct. Mater. 29 (17) (2019), https://doi.org/10.1002/adfm.201806306.
[7] R. Pandiyan, S. Mahalingam, Y.-H. Ahn, Antibacterial and photocatalytic activity of hydrothermally synthesized SnO2 doped GO and CNT under visible light irradiation, J. Photochem. Photobiol. B Biol. 191 (2019) 18–25, https://doi.org/10.1016/j.jphotobiol.2018.12.007.
[8] Z. Yin, C. Cui, H. Chen, X. Yu, W. Qian, The application of carbon nanotube/graphene-based nanomaterials in wastewater treatment, Small 16 (15) (2020), 1902301, https://doi.org/10.1002/smll.201902301.
[9] M. Salehi, Z. Shariatinia, A. Sadeghi, Application of RGO/CNT nanocomposite as cathode material in lithium-air battery, J. Electroanal. Chem. 832 (2019) 165–173, https://doi.org/10.1016/j.jelechem.2018.10.053.
[10] N. Liu, Y. Liu, Y. Zhao, Y. Liu, Q. Lan, J. Qin, Z. Song, H. Zhan, CNT-intertwined polymer electrode toward the practical application of wearable devices, ACS Appl. Mater. Interfaces 11 (50) (2019) 46726–46734, https://doi.org/10.1021/acsami.9b15462.
[11] C. Wang, S. Yang, Q. Ma, X. Jia, P.-C. Ma, Preparation of carbon nanotubes/graphene hybrid aerogel and its application for the adsorption of organic compounds, Carbon 118 (2017) 765–771, https://doi.org/10.1016/j.carbon.2017.04.001.
[12] A. Kumar, K. Sharma, A.R. Dixit, A review on the mechanical and thermal properties of graphene and graphene-based polymer nanocomposites: understanding of modelling and MD simulation, Mol. Simulat. 46 (2) (2020) 136–154, https://doi.org/10.1080/08927022.2019.1680844.
[13] A. Kumar, K. Sharma, A.R. Dixit, A review of the mechanical and thermal properties of graphene and its hybrid polymer nanocomposites for structural applications, J. Mater. Sci. 54 (8) (2019) 5992–6026, https://doi.org/10.1007/s10853-018-03244-3.
[14] D. Zhi, T. Li, J. Li, H. Ren, F. Meng, A review of three-dimensional graphene-based aerogels: synthesis, structure and application for microwave absorption, Compos. B Eng. (2021), 108642, https://doi.org/10.1016/j.compositesb.2021.108642.
[15] Q. Yang, Y. Qian, Z. Fan, J. Lin, D. Wang, J. Zhong, M. Oeser, Exploiting the synergetic effects of graphene and carbon nanotubes on the mechanical properties of bitumen composites, Carbon 172 (2021) 402–413, https://doi.org/10.1016/j.carbon.2020.10.020.
[16] G. Yang, X. Feng, W. Wang, Q. OuYang, L. Liu, Z. Wu, Graphene and carbon nanotube-based high-sensitive film sensors for in-situ monitoring out-of-plane shear damage of epoxy composites, Compos. B Eng. 204 (2021), 108494, https://doi.org/10.1016/j.compositesb.2020.108494.
[17] T. Shiraki, Molecular functionalization of carbon nanotubes towards near infrared photoluminescent nanomaterials, Chem. Lett. 50 (X) (2021), https://doi.org/10.1246/cl.200776.
[18] A. Sharma, G. Gupta, J. Paul, A comprehensive review on the dispersion and survivability issues of carbon nanotubes in Al/CNT nanocomposites fabricated via friction stir processing, Carbon Lett. (2021) 1–32, https://doi.org/10.1007/s42823-020-00207-0.
[19] V. Khanna, V. Kumar, S.A. Bansal, Mechanical properties of aluminium-graphene/carbon nanotubes (CNTs) metal matrix composites: advancement, opportunities and perspective, Mater. Res. Bull. 138 (2021), 111224, https://doi.org/10.1016/j.materresbull.2021.111224.
[20] B. Fu, P. Ren, Z. Guo, Z. Zong, Y. Jin, Z. Dai, F. Ren, Preparation of porous graphene nanosheets/carbon nanotube/polyvinylidene fluoride (GNS/CNT/PVDF) composites for high microwave absorption in X-band, J. Mater. Sci. Mater. Electron. 32 (7) (2021) 9611–9622, https://doi.org/10.1007/s10854-021-05623-0.
[21] N.F. Braga, H. Ding, L. Sun, F.R. Passador, Antistatic packaging based on PTT/PTT-g-MA/ABS/MWCNT nanocomposites: effect of the chemical functionalization of MWCNTs, J. Appl. Polym. Sci. 138 (11) (2021), 50005, https://doi.org/10.1002/app.50005.
[22] S. Araby, B. Philips, Q. Meng, J. Ma, T. Laoui, C.H. Wang, Recent advances in carbon-based nanomaterials for flame retardant polymers and composites, Compos. B Eng. (2021), 108675, https://doi.org/10.1016/j.compositesb.2021.108675.
[23] S. Iijima, T. Ichihashi, SINGLE-SHELL carbon nanotubes OF 1-NM diameter, Nature 363 (6430) (1993) 603–605, https://doi.org/10.1038/363603a0.
[24] S. Iijima, Helical microtubules OF graphitic carbon, Nature 354 (6348) (1991) 56–58, https://doi.org/10.1038/354056a0.
[25] Y.L. Lu, J. Liu, G.Y. Hou, J. Ma, W.C. Wang, F. Wei, L.Q. Zhang, From nano to giant? Designing carbon nanotubes for rubber reinforcement and their applications for high performance tires, Compos. Sci. Technol. 137 (2016) 94–101, https://doi.org/10.1016/j.compscitech.2016.10.020.
[26] K.S. Novoselov, A.K. Geim, S.V. Morozov, D. Jiang, Y. Zhang, S.V. Dubonos, I.V. Grigorieva, A.A. Firsov, Electric field effect in atomically thin carbon films, Science 306 (5696) (2004) 666–669, https://doi.org/10.1126/science.1102896.
[27] C.A. Marianetti, H.G. Yevick, Failure mechanisms of graphene under tension, Phys. Rev. Lett. 105 (24) (2010) 245502, https://doi.org/10.1103/PhysRevLett.105.245502.
[28] A. Liang, X. Jiang, X. Hong, Y. Jiang, Z. Shao, D. Zhu, Recent developments concerning the dispersion methods and mechanisms of graphene, Coatings 8 (1) (2018) 33, https://doi.org/10.3390/coatings8010033.
[29] T.-Y. Sun, Y. Hao, C.-T. Lin, L. Wang, L.-F. Huang, Unraveling the strong coupling between graphene/nickel interface and atmospheric adsorbates for versatile realistic applications, Carbon Trends 2 (2021), 100013, https://doi.org/10.1016/j.cartre.2020.100013.
[30] A. Radhi, D. Mohamad, F.S.A. Rahman, A.M. Abdullah, H. Hasan, Mechanism and factors influence of graphene-based nanomaterials antimicrobial activities and application in dentistry, J. Mater. Res. Technol. (2021), https://doi.org/10.1016/j.jmrt.2021.01.093.
[31] S. Rumyantsev, G. Liu, W. Stillman, M. Shur, A. Balandin, Electrical and noise characteristics of graphene field-effect transistors: ambient effects, noise sources and physical mechanisms, J. Phys. Condens. Matter 22 (39) (2010), 395302, https://doi.org/10.1088/0953-8984/22/39/395302.
[32] X. Xia, J. Hao, Y. Wang, Z. Zhong, G.J. Weng, Theory of electrical conductivity and dielectric permittivity of highly aligned graphene-based nanocomposites, J. Phys. Condens. Matter 29 (20) (2017), 205702, https://doi.org/10.1088/1361-648X/aa68ec.
[33] E. Kandare, A.A. Khatibi, S. Yoo, R. Wang, J. Ma, P. Olivier, N. Gleizes, C.H. Wang, Improving the through-thickness thermal and electrical conductivity of carbon fibre/epoxy laminates by exploiting synergy between graphene and silver nano-inclusions, Compos. Appl. Sci. Manuf. 69 (2015) 72–82, https://doi.org/10.1016/j.compositesa.2014.10.024.
[34] M. Kaseem, K. Hamad, Y.G. Ko, Fabrication and materials properties of polystyrene/carbon nanotube (PS/CNT) composites: a review, Eur. Polym. J. 79 (2016) 36–62, https://doi.org/10.1016/j.eurpolymj.2016.04.011.
[35] B.-G. Cho, J.-E. Lee, S.-H. Hwang, J.H. Han, H.G. Chae, Y.-B. Park, Enhancement in mechanical properties of polyamide 66-carbon fiber composites containing graphene oxide-carbon nanotube hybrid nanofillers synthesized through in situ interfacial polymerization, Compos. Appl. Sci. Manuf. 135 (2020), 105938, https://doi.org/10.1016/j.compositesa.2020.105938.
[36] J. Ma, L.T.B. La, I. Zaman, Q.S. Meng, L. Luong, D. Ogilvie, H.C. Kuan, Fabrication, structure and properties of epoxy/metal nanocomposites, Macromol. Mater. Eng. 296 (5) (2011) 465–474, https://doi.org/10.1002/mame.201000409.
[37] Q.S. Meng, H. Wu, Z.H. Zhao, S. Araby, S.W. Lu, J. Ma, Free-standing, flexible, electrically conductive epoxy/graphene composite films, Compos. Appl. Sci. Manuf. 92 (2017) 42–50, https://doi.org/10.1016/j.compositesa.2016.10.028.
[38] Y.Z. Keteklahijani, A.S. Zeraati, F. Sharif, E.P. Roberts, U. Sundararaj, In situ chemical polymerization of conducting polymer nanocomposites: effect of DNA-functionalized carbon nanotubes and nitrogen-doped graphene as catalytic molecular templates, Chem. Eng. J. 389 (2020), 124500, https://doi.org/10.1016/j.cej.2020.124500.
[39] N. Pongpichayakul, P. Waenkeaw, J. Jakmunee, S. Themsirimongkon, S. Saipanya, Activity and stability improvement of platinum loaded on reduced graphene oxide and carbon nanotube composites for methanol oxidation, J. Appl. Electrochem. 50 (1) (2020) 51–62, https://doi.org/10.1007/s10800-019-01368-1.
[40] A. Bisht, K. Dasgupta, D. Lahiri, Evaluating the effect of addition of nanodiamond on the synergistic effect of graphene-carbon nanotube hybrid on the mechanical properties of epoxy based composites, Polym. Test. 81 (2020), 106274, https://doi.org/10.1016/j.polymertesting.2019.106274.
[41] J. Ma, H. Xu, J.H. Ren, Z.Z. Yu, Y.W. Mai, A new approach to polymer/montmorillonite nanocomposites, Polymer 44 (16) (2003) 4619–4624, https://doi.org/10.1016/s0032-3861(03)00362-8.
[42] S. Dul, L.G. Ecco, A. Pegoretti, L. Fambri, Graphene/carbon nanotube hybrid nanocomposites: effect of compression molding and fused filament fabrication on properties, Polymers 12 (1) (2020) 101, https://doi.org/10.3390/polym12010101.
[43] S. Araby, Q.S. Meng, L.Q. Zhang, H.L. Kang, P. Majewski, Y.H. Tang, J. Ma, Electrically and thermally conductive elastomer/graphene nanocomposites by solution mixing, Polymer 55 (1) (2014) 201–210, https://doi.org/10.1016/j.polymer.2013.11.032.
[44] R. Wang, H.-C. Kuan, A. Qiu, X. Su, J. Ma, A facile approach to the scalable preparation of thermoplastic/carbon nanotube composites, Nanotechnology 31 (19) (2020), 195706, https://doi.org/10.1088/1361-6528/ab5a28.
[45] Q.S. Meng, H.C. Kuan, S. Araby, N. Kawashima, N. Saber, C.H. Wang, J. Ma, Effect of interface modification on PMMA/graphene nanocomposites, J. Mater. Sci. 49 (17) (2014) 5838–5849, https://doi.org/10.1007/s10853-014-8278-0.
[46] S. Araby, C.H. Wang, H. Wu, Q.S. Meng, H.C. Kuan, N.K. Kim, A. Mouritz, J. Ma, Development of flame-retarding elastomeric composites with high mechanical performance, Compos. Appl. Sci. Manuf. 109 (2018) 257–266, https://doi.org/10.1016/j.compositesa.2018.03.012.
[47] S. Araby, X. Su, Q.S. Meng, H.C. Kuan, C.H. Wang, A. Mouritz, A. Maged, J. Ma, Graphene platelets versus phosphorus compounds for elastomeric composites: flame retardancy, mechanical performance and mechanisms, Nanotechnology 30 (38) (2019), https://doi.org/10.1088/1361-6528/ab2a3d.
[48] W.N.W. Busu, R.S. Chen, M.J.M. Yusof, S. Ahmad, Graphene enhanced linear low-density polyethylene nanocomposites by premixing and melt compounding, J. Metals, Mater. Min. 31 (1) (2021), https://doi.org/10.14456/jmmm.2021.2.
[49] A. Alvaredo-Atienza, J.P. Fernández-Blázquez, P. Castell, R.G. de Villoria, Production of graphene nanoplate/polyetheretherketone composites by semi-industrial melt-compounding, Heliyon 6 (4) (2020), e03740, https://doi.org/10.1016/j.heliyon.2020.e03740.
[50] S. Araby, I. Zaman, Q.S. Meng, N. Kawashima, A. Michelmore, H.C. Kuan, P. Majewski, J. Ma, L.Q. Zhang, Melt compounding with graphene to develop

functional, high-performance elastomers, Nanotechnology 24 (16) (2013), https://doi.org/10.1088/0957-4484/24/16/165601.
[51] S. Araby, N. Saber, X. Ma, N. Kawashima, H.L. Kang, H. Shen, L.Q. Zhang, J. Xu, P. Majewski, J. Ma, Implication of multi-walled carbon nanotubes on polymer/graphene composites, Mater. Des. 65 (2015) 690–699, https://doi.org/10.1016/j.matdes.2014.09.069.
[52] S. Araby, Q.S. Meng, L.Q. Zhang, I. Zaman, P. Majewski, J. Ma, Elastomeric composites based on carbon nanomaterials, Nanotechnology 26 (11) (2015), https://doi.org/10.1088/0957-4484/26/11/112001.
[53] F. Li, Y.L. Lu, L. Liu, L.Q. Zhang, J.B. Dai, J. Ma, Relations between carbon nanotubes' length and their composites' mechanical and functional performance, Polymer 54 (8) (2013) 2158–2165, https://doi.org/10.1016/j.polymer.2013.02.019.
[54] I.A. Kinloch, J. Suhr, J. Lou, R.J. Young, P.M. Ajayan, Composites with carbon nanotubes and graphene: an outlook, Science 362 (6414) (2018) 547–553, https://doi.org/10.1126/science.aat7439.
[55] Z. Zhang, Y. Li, H.L. Wu, H.Q. Zhang, H.P. Wu, S.F. Jiang, G.Z. Chai, Mechanical analysis of functionally graded graphene oxide-reinforced composite beams based on the first-order shear deformation theory, Mech. Adv. Mater. Struct. 27 (1) (2020) 3–11, https://doi.org/10.1080/15376494.2018.1444216.
[56] L.T.N. Trang, H.V. Tung, Nonlinear stability of CNT-reinforced composite cylindrical panels with elastically restrained straight edges under combined thermomechanical loading conditions, J. Thermoplast. Compos. Mater. 33 (2) (2020) 153–179, https://doi.org/10.1177/0892705718805134.
[57] S. Choi, S.I. Han, D. Kim, T. Hyeon, D.H. Kim, High-performance stretchable conductive nanocomposites: materials, processes, and device applications, Chem. Soc. Rev. 48 (6) (2019) 1566–1595, https://doi.org/10.1039/c8cs00706c.
[58] P. Sonia, J.K. Jain, P. Singhal, K.K. Saxena, Performance evaluation of hybrid polymer nanocomposite, Mater. Today: Proc. (2021), https://doi.org/10.1016/j.matpr.2020.11.826.
[59] F. Najafi, G. Wang, S. Mukherjee, T. Cui, T. Filleter, C.V. Singh, Toughening of graphene-based polymer nanocomposites via tuning chemical functionalization, Compos. Sci. Technol. 194 (2020), 108140, https://doi.org/10.1016/j.compscitech.2020.108140.
[60] A. Kumar, K. Sharma, A.R. Dixit, A review on the mechanical properties of polymer composites reinforced by carbon nanotubes and graphene, Carbon Lett. (2020) 1–17, https://doi.org/10.1007/s42823-020-00161-x.
[61] R. Gholami, H. Khoramishad, L.F. da Silva, Glass fiber-reinforced polymer nanocomposite adhesive joints reinforced with aligned carbon nanofillers, Compos. Struct. 253 (2020), 112814, https://doi.org/10.1016/j.compstruct.2020.112814.
[62] G.Q. Li, J.E. Helms, S.S. Pang, K. Schulz, Analytical modeling of tensile strength of particulate-filled composites, Polym. Compos. 22 (5) (2001) 593–603, https://doi.org/10.1002/pc.10562.
[63] Q.H. Le, H.C. Kuan, J.B. Dai, I. Zaman, L. Luong, J. Ma, Structure-property relations of 55 nm particle-toughened epoxy, Polymer 51 (21) (2010) 4867–4879, https://doi.org/10.1016/j.polymer.2010.08.038.
[64] Z.W. Pan, S.S. Xie, B.H. Chang, C.Y. Wang, L. Lu, W. Liu, M.Y. Zhou, W.Z. Li, Very long carbon nanotubes, Nature 394 (6694) (1998) 631–632, https://doi.org/10.1038/29206.
[65] J. Chen, M.A. Hamon, H. Hu, Y.S. Chen, A.M. Rao, P.C. Eklund, R.C. Haddon, Solution properties of single-walled carbon nanotubes, Science 282 (5386) (1998) 95–98, https://doi.org/10.1126/science.282.5386.95.
[66] D.G. Papageorgiou, Z.L. Li, M.F. Liu, I.A. Kinloch, R.J. Young, Mechanisms of mechanical reinforcement by graphene and carbon nanotubes in polymer nanocomposites, Nanoscale 12 (4) (2020) 2228–2267, https://doi.org/10.1039/c9nr06952f.
[67] B. Safadi, R. Andrews, E.A. Grulke, Multiwalled carbon nanotube polymer composites: synthesis and characterization of thin films, J. Appl. Polym. Sci. 84 (14) (2002) 2660–2669, https://doi.org/10.1002/app.10436.
[68] M.F.L. De Volder, S.H. Tawfick, R.H. Baughman, A.J. Hart, Carbon nanotubes: present and future commercial applications, Science 339 (6119) (2013) 535–539, https://doi.org/10.1126/science.1222453.
[69] S.Q. Li, F. Wang, Y. Wang, J.W. Wang, J. Ma, J. Xiao, Effect of acid and TETA modification on mechanical properties of MWCNTs/epoxy composites, J. Mater. Sci. 43 (8) (2008) 2653–2658, https://doi.org/10.1007/s10853-008-2489-1.
[70] A. Thess, R. Lee, P. Nikolaev, H.J. Dai, P. Petit, J. Robert, C.H. Xu, Y.H. Lee, S.G. Kim, A.G. Rinzler, D.T. Colbert, G.E. Scuseria, D. Tomanek, J.E. Fischer, R.E. Smalley, Crystalline ropes of metallic carbon nanotubes, Science 273 (5274) (1996) 483–487, https://doi.org/10.1126/science.273.5274.483.
[71] J. Ma, Y.X. Feng, J. Xu, M.L. Xiong, Y.J. Zhu, L.Q. Zhang, Effects of compatibilizing agent and in situ fibril on the morphology, interface and mechanical properties of EPDM/nylon copolymer blends, Polymer 43 (3) (2002) 937–945, https://doi.org/10.1016/s0032-3861(01)00626-7.
[72] R.S. Rajaura, S. Srivastava, P.K. Sharma, S. Mathur, R. Shrivastava, S. Sharma, Y. Vijay, Structural and surface modification of carbon nanotubes for enhanced hydrogen storage density, Nano-Struct. Nano-Objects 14 (2018) 57–65, https://doi.org/10.1016/j.nanoso.2018.01.005.
[73] N. Mohd Nurazzi, M. Muhammad Asyraf, A. Khalina, N. Abdullah, F.A. Sabaruddin, S.H. Kamarudin, S. Ahmad, A.M. Mahat, C.L. Lee, H. Aisyah, Fabrication, functionalization, and application of carbon nanotube-reinforced polymer composite: an overview, Polymers 13 (7) (2021) 1047, https://doi.org/10.3390/polym13071047.
[74] J. Chen, L. Yan, W. Song, D. Xu, Interfacial characteristics of carbon nanotube-polymer composites: a review, Compos. Appl. Sci. Manuf. 114 (2018) 149–169, https://doi.org/10.1016/j.compositesa.2018.08.021.
[75] Y. Zhou, Y. Fang, R.P. Ramasamy, Non-covalent functionalization of carbon nanotubes for electrochemical biosensor development, Sensors 19 (2) (2019), https://doi.org/10.3390/s19020392.
[76] M.S. Ata, R. Poon, A.M. Syed, J. Milne, I. Zhitomirsky, New developments in non-covalent surface modification, dispersion and electrophoretic deposition of carbon nanotubes, Carbon 130 (2018) 584–598, https://doi.org/10.1016/j.carbon.2018.01.066.
[77] M. Sianipar, S.H. Kim, Khoiruddin, F. Iskandar, I.G. Wenten, Functionalized carbon nanotube (CNT) membrane: progress and challenges, RSC Adv. 7 (81) (2017) 51175–51198, https://doi.org/10.1039/c7ra08570b.
[78] T. Fujigaya, N. Nakashima, Non-covalent polymer wrapping of carbon nanotubes and the role of wrapped polymers as functional dispersants, Sci. Technol. Adv. Mater. 16 (2) (2015), https://doi.org/10.1088/1468-6996/16/2/024802.
[79] S.J. Chen, C.Y. Qiu, A.H. Korayem, M.R. Barati, W.H. Duan, Agglomeration process of surfactant-dispersed carbon nanotubes in unstable dispersion: a two-stage agglomeration model and experimental evidence, Powder Technol. 301 (2016) 412–420, https://doi.org/10.1016/j.powtec.2016.06.033.
[80] J.N. Coleman, U. Khan, W.J. Blau, Y.K. Gun'ko, Small but strong: a review of the mechanical properties of carbon nanotube-polymer composites, Carbon 44 (9) (2006) 1624–1652, https://doi.org/10.1016/j.carbon.2006.02.038.
[81] K.M. Liew, M.F. Kai, L.W. Zhang, Carbon nanotube reinforced cementitious composites: an overview, Compos. Appl. Sci. Manuf. 91 (2016) 301–323, https://doi.org/10.1016/j.compositesa.2016.10.020.
[82] R.Q. He, Q.X. Chang, C.Z. Peng, The improvement in interfacial shear strength of wood fiber/epoxy composite by sizing with epoxy sizing agent containing MWCNTs, Surf. Interface Anal. 50 (8) (2018) 807–812, https://doi.org/10.1002/sia.6482.
[83] P. Smolen, T. Czujko, Z. Komorek, D. Grochala, A. Rutkowska, M. Osiewicz-Powezka, Mechanical and electrical properties of epoxy composites modified by functionalized multiwalled carbon nanotubes, Materials (2021) 1573, https://doi.org/10.3390/ma14123325, 3325.
[84] R. Razavi, Y. Zare, K.Y. Rhee, A model for tensile strength of polymer/carbon nanotubes nanocomposites assuming the percolation of interphase regions, Colloid. Surface. Physicochem. Eng. Aspect. 538 (2018) 148–154, https://doi.org/10.1016/j.colsurfa.2017.10.063.
[85] G. Pal, S. Kumar, Modeling of carbon nanotubes and carbon nanotube-polymer composites, Prog. Aero. Sci. 80 (2016) 33–58, https://doi.org/10.1016/j.paerosci.2015.12.001.
[86] M. Meo, M. Rossi, Prediction of Young's modulus of single wall carbon nanotubes by molecular-mechanics based finite element modelling, Compos. Sci. Technol. 66 (11–12) (2006) 1597–1605, https://doi.org/10.1016/j.compscitech.2005.11.015.
[87] D.G. Papageorgiou, Z. Li, M. Liu, I.A. Kinloch, R.J. Young, Mechanisms of mechanical reinforcement by graphene and carbon nanotubes in polymer nanocomposites, Nanoscale 12 (4) (2020) 2228–2267, https://doi.org/10.1039/c9nr06952f.
[88] Y. Zare, K.Y. Rhee, Tensile strength prediction of carbon nanotube reinforced composites by expansion of cross-orthogonal skeleton structure, Compos. B Eng. 161 (2019) 601–607, https://doi.org/10.1016/j.compositesb.2019.01.001.
[89] Y. Zare, K.Y. Rhee, S.J. Park, A developed equation for electrical conductivity of polymer carbon nanotubes (CNT) nanocomposites based on Halpin-Tsai model, Res. Phys. 14 (2019), https://doi.org/10.1016/j.rinp.2019.102406.
[90] M.K. Hassanzadeh-Aghdam, J. Jamali, A new form of a Halpin-Tsai micromechanical model for characterizing the mechanical properties of carbon nanotube-reinforced polymer nanocomposites, Bull. Mater. Sci. 42 (3) (2019), https://doi.org/10.1007/s12034-019-1784-6.
[91] F. Aghadavoudi, H. Golestanian, Y.T. Beni, Investigating the effects of CNT aspect ratio and agglomeration on elastic constants of crosslinked polymer nanocomposite using multiscale modeling, Polym. Compos. 39 (12) (2018) 4513–4523, https://doi.org/10.1002/pc.24557.
[92] Y. Zare, K.Y. Rhee, The mechanical behavior of CNT reinforced nanocomposites assuming imperfect interfacial bonding between matrix and nanoparticles and percolation of interphase regions, Compos. Sci. Technol. 144 (2017) 18–25, https://doi.org/10.1016/j.compscitech.2017.03.012.
[93] M.M. Shokrieh, H. Moshrefzadeh-Sani, On the constant parameters of Halpin-Tsai equation, Polymer 106 (2016) 14–20, https://doi.org/10.1016/j.polymer.2016.10.049.
[94] M.M. Shokrieh, A. Saeedi, M. Chitsazzadeh, Mechanical properties of multi-walled carbon nanotube/polyester nanocomposites, J. Nanostruct. Chem. 3 (1) (2013) 1–5, https://doi.org/10.1186/2193-8865-3-20.
[95] A.A. Sapalidis, P.I. Karantzis, A. Vairis, S.F. Nitodas, S. Barbe, E.P. Favvas, A study of the reinforcement effect of MWCNTs onto polyimide flat sheet membranes, Polymers 12 (6) (2020) 1381, https://doi.org/10.3390/polym12061381.
[96] T. Xu, Z. Qi, Y. Tan, J. Tian, X. Li, Effect of multiwalled carbon nanotube diameter on mechanical behavior and fracture toughness of epoxy nanocomposites, Mater. Res. Express 8 (1) (2021), 015014, https://doi.org/10.1088/2053-1591/abd864.
[97] H. Hosseini, H. Mahdavi, Nanocomposite based on epoxy and MWCNTs modified with NiFe2O4 nanoparticles as efficient microwave absorbing material, Appl. Organomet. Chem. 32 (4) (2018), e4294, https://doi.org/10.1002/aoc.4294.
[98] F.V. Ferreira, B.R.C. Menezes, W. Franceschi, E.V. Ferreira, K. Lozano, L.S. Cividanes, A.R. Coutinho, G.P. Thim, Influence of carbon nanotube concentration and sonication temperature on mechanical properties of HDPE/CNT nanocomposites, Fullerenes, Nanotub. Carbon Nanostruct. 25 (9) (2017) 531–539, https://doi.org/10.1080/1536383x.2017.1359553.
[99] E. Bazireh, M. Sharif, Polythiophene-coated multi-walled carbon nanotube-reinforced epoxy nanocomposites for enhanced mechanical, electrical and thermal

properties, Polym. Bull. 77 (9) (2020) 4537–4553, https://doi.org/10.1007/s00289-019-02981-y.
[100] L. Mohan, P.N. Kumar, S. Karakkad, S.T. Krishnan, Determination of electrical percolation threshold of carbon nanotube-based epoxy nanocomposites and its experimental validation, IET Sci. Meas. Technol. 13 (9) (2019) 1299–1304, https://doi.org/10.1049/iet-smt.2019.0011.
[101] A.S. Babal, R. Gupta, B.P. Singh, V.N. Singh, S.R. Dhakate, R.B. Mathur, Mechanical and electrical properties of high performance MWCNT/polycarbonate composites prepared by an industrial viable twin screw extruder with back flow channel, RSC Adv. 4 (110) (2014) 64649–64658, https://doi.org/10.1039/c4ra11319e.
[102] A. Mirsamiei, K. Faghihi, M. Shabanian, Synthesis and studies of thermal, mechanical and electrical properties of MWCNT-cyclodextrin as a nanoparticle in polyamide matrix based on 2,2-Bis 4-(4-aminophenoxy)phenyl propane, Polym. Adv. Technol. 28 (7) (2017) 779–790, https://doi.org/10.1002/pat.3978.
[103] O.B. Mergen, E. Arda, G.A. Evingur, Electrical, mechanical, and optical changes in MWCNT-doped PMMA composite films, J. Compos. Mater. 54 (18) (2020) 2449–2459, https://doi.org/10.1177/0021998319898507.
[104] Z.I. Lin, C.W. Lou, Y.J. Pan, C.T. Hsieh, C.L. Huang, C.H. Huang, Y.S. Chen, J.H. Lin, The effects of MWCNT length on the mechanical, crystallization and electromagnetic interference shielding effectiveness of PP/MWCNT composites, J. Polym. Res. 24 (2) (2017), https://doi.org/10.1007/s10965-016-1121-3.
[105] S. Dabees, V. Tirth, A. Mohamed, B.M. Kamel, Wear performance and mechanical properties of MWCNT/HDPE nanocomposites for gearing applications, J. Mater. Res. Technol. Jmr T 12 (2021) 2476–2488, https://doi.org/10.1016/j.jmrt.2020.09.129.
[106] P. Bernal-Ortega, M.M. Bernal, A. González-Jiménez, P. Posadas, R. Navarro, J.L. Valentín, New insight into structure-property relationships of natural rubber and styrene-butadiene rubber nanocomposites filled with MWCNT, Polymer 201 (2020), 122604, https://doi.org/10.1016/j.polymer.2020.122604.
[107] M. Liebscher, T. Gartner, L. Tzounis, M. Micusik, P. Potschke, M. Stamm, G. Heinrich, B. Voit, Influence of the MWCNT surface functionalization on the thermoelectric properties of melt-mixed polycarbonate composites, Compos. Sci. Technol. 101 (2014) 133–138, https://doi.org/10.1016/j.compscitech.2014.07.009.
[108] M.H. Al-Saleh, Influence of polymer structure on the electrical resistivity of nanocomposite materials, Synth. Met. 265 (2020), https://doi.org/10.1016/j.synthmet.2020.116409.
[109] J.M. Bressanin, V.A. Assis, J.R. Bartoli, Electrically conductive nanocomposites of PMMA and carbon nanotubes prepared by in situ polymerization under probe sonication, Chem. Pap. 72 (7) (2018) 1799–1810, https://doi.org/10.1007/s11696-018-0443-5.
[110] F.F. Tao, L. Bonnaud, O. Murariu, D. Auhl, P. Dubois, C. Bailly, A convenient route to high-performance HDPE-CNT conductive nanocomposites by control of matrix nucleation, Macromol. Chem. Phys. 213 (21) (2012) 2275–2281, https://doi.org/10.1002/macp.201200477.
[111] L.N. Shao, J. Chen, J. Dai, H.M. Chen, J.H. Yang, Y. Wang, C.L. Zhang, Morphology, rheology and electrical resistivity of PLLA/HDPE/CNT nanocomposites: effect of maleic anhydride, Mater. Chem. Phys. 152 (2015) 104–112, https://doi.org/10.1016/j.matchemphys.2014.12.020.
[112] H. Wang, K. Kurata, T. Fukunaga, H. Ago, H. Takamatsu, X. Zhang, T. Ikuta, K. Takahashi, T. Nishiyama, Y. Takata, Simultaneous measurement of electrical and thermal conductivities of suspended monolayer graphene, J. Appl. Phys. 119 (24) (2016), 244306, https://doi.org/10.1063/1.4954677.
[113] Q. Meng, J. Jin, R. Wang, H.-C. Kuan, J. Ma, N. Kawashima, A. Michelmore, S. Zhu, C.H. Wang, Processable 3-nm thick graphene platelets of high electrical conductivity and their epoxy composites, Nanotechnology 25 (12) (2014), 125707, https://doi.org/10.1088/0957-4484/25/12/125707.
[114] I. Ovid'Ko, Mechanical properties of graphene, Rev. Adv. Mater. Sci. 34 (1) (2013) 1–11. https://www.ipme.ru/e-journals/RAMS/no_13413/01_13413_ovidko.pdf.
[115] I. Zaman, H.-C. Kuan, Q. Meng, A. Michelmore, N. Kawashima, T. Pitt, L. Zhang, S. Gouda, L. Luong, J. Ma, A facile approach to chemically modified graphene and its polymer nanocomposites, Adv. Funct. Mater. 22 (13) (2012) 2735–2743, https://doi.org/10.1002/adfm.201103041.
[116] I. Zaman, H.C. Kuan, J.F. Dai, N. Kawashima, A. Michelmore, A. Sovi, S.Y. Dong, L. Luong, J. Ma, From carbon nanotubes and silicate layers to graphene platelets for polymer nanocomposites, Nanoscale 4 (15) (2012) 4578–4586, https://doi.org/10.1039/c2nr30837a.
[117] I. Zaman, B. Manshoor, A. Khalid, S. Araby, From clay to graphene for polymer nanocomposites-a survey, J. Polym. Res. 21 (5) (2014), https://doi.org/10.1007/s10965-014-0429-0.
[118] I. Zaman, B. Manshoor, A. Khalid, Q.S. Meng, S. Araby, Interface modification of clay and graphene platelets reinforced epoxy nanocomposites: a comparative study, J. Mater. Sci. 49 (17) (2014) 5856–5865, https://doi.org/10.1007/s10853-014-8296-y.
[119] I. Zaman, T.T. Phan, H.C. Kuan, Q.S. Meng, L.T.B. La, L. Luong, O. Youssf, J. Ma, Epoxy/graphene platelets nanocomposites with two levels of interface strength, Polymer 52 (7) (2011) 1603–1611, https://doi.org/10.1016/j.polymer.2011.02.003.
[120] R. Raccichini, A. Varzi, S. Passerini, B. Scrosati, The role of graphene for electrochemical energy storage, Nat. Mater. 14 (3) (2015) 271–279, https://doi.org/10.1038/nmat4170.
[121] P.R. Somani, S.P. Somani, M. Umeno, Planer nano-graphenes from camphor by CVD, Chem. Phys. Lett. 430 (1–3) (2006) 56–59, https://doi.org/10.1016/j.cplett.2006.06.081.
[122] Z.Y. Cai, B.L. Liu, X.L. Zou, H.M. Cheng, Chemical vapor deposition growth and applications of two-dimensional materials and their heterostructures, Chem. Rev. 118 (13) (2018) 6091–6133, https://doi.org/10.1021/acs.chemrev.7b00536.
[123] Y.H. Xu, J.Q. Liu, Graphene as transparent electrodes: fabrication and new emerging applications, Small 12 (11) (2016) 1400–1419, https://doi.org/10.1002/smll.201502988.
[124] M.S.A. Bhuyan, M.N. Uddin, M.M. Islam, F.A. Bipasha, S.S. Hossain, Synthesis of graphene, Int. Nano Lett. 6 (2) (2016) 65–83, https://doi.org/10.1007/s40089-015-0176-1.
[125] A. Hussain, S.M. Mehdi, N. Abbas, M. Hussain, R.A. Naqvi, Synthesis of graphene from solid carbon sources: a focused review, Mater. Chem. Phys. 248 (2020), https://doi.org/10.1016/j.matchemphys.2020.122924.
[126] W. Hummers, R. Offeman, Graphene oxide, JACS 80 (6) (1958) 1339, https://doi.org/10.1021/ja01539a017.
[127] W.S. Hummers Jr., R.E. Offeman, Preparation of graphitic oxide, J. Am. Chem. Soc. 80 (6) (1958), https://doi.org/10.1021/ja01539a017, 1339-1339.
[128] S. Yadav, N. Goel, V. Kumar, K. Tikoo, S. Singhal, Removal of fluoroquinolone from aqueous solution using graphene oxide: experimental and computational elucidation, Environ. Sci. Pollut. Control Ser. 25 (3) (2018) 2942–2957, https://doi.org/10.1007/s11356-017-0596-8.
[129] S. Sadhukhan, T.K. Ghosh, D. Rana, I. Roy, A. Bhattacharyya, G. Sarkar, M. Chakraborty, D. Chattopadhyay, Studies on synthesis of reduced graphene oxide (RGO) via green route and its electrical property, Mater. Res. Bull. 79 (2016) 41–51, https://doi.org/10.1016/j.materresbull.2016.02.039.
[130] R.K. Singh, R. Kumar, D.P. Singh, Graphene oxide: strategies for synthesis, reduction and frontier applications, RSC Adv. 6 (69) (2016) 64993–65011, https://doi.org/10.1039/c6ra07626b.
[131] D. Voiry, J. Yang, J. Kupferberg, R. Fullon, C. Lee, H.Y. Jeong, H.S. Shin, M. Chhowalla, High-quality graphene via microwave reduction of solution-exfoliated graphene oxide, Science 353 (6306) (2016) 1413–1416, https://doi.org/10.1126/science.aah3398.
[132] K.M. Shahil, A.A. Balandin, Thermal properties of graphene and multilayer graphene: applications in thermal interface materials, Solid State Commun. 152 (15) (2012) 1331–1340, https://doi.org/10.1016/j.ssc.2012.04.034.
[133] Q.S. Meng, J. Jin, R.Y. Wang, H.C. Kuan, J. Ma, N. Kawashima, A. Michelmore, S.M. Zhu, C.H. Wang, Processable 3-nm thick graphene platelets of high electrical conductivity and their epoxy composites, Nanotechnology 25 (12) (2014), https://doi.org/10.1088/0957-4484/25/12/125707.
[134] J. Ma, Q.S. Meng, A. Michelmore, N. Kawashima, Z. Izzuddin, C. Bengtsson, H.C. Kuan, Covalently bonded interfaces for polymer/graphene composites, J. Mater. Chem. 1 (13) (2013) 4255–4264, https://doi.org/10.1039/c3ta01277h.
[135] J. Ma, Q.S. Meng, I. Zaman, S.M. Zhu, A. Michelmore, N. Kawashima, C.H. Wang, H.C. Kuan, Development of polymer composites using modified, high-structural integrity graphene platelets, Compos. Sci. Technol. 91 (2014) 82–90, https://doi.org/10.1016/j.compscitech.2013.11.017.
[136] M. Naeem, H.C. Kuan, A. Michelmore, S.R. Yu, A.P. Mouritz, S.S. Chelliah, J. Ma, Epoxy/graphene nanocomposites prepared by in-situ microwaving, Carbon 177 (2021) 271–281, https://doi.org/10.1016/j.carbon.2021.02.059.
[137] J. Ma, Q. Qi, J. Bayley, X.S. Du, M.S. Mo, L.Q. Zhang, Development of SENB toughness measurement for thermoset resins, Polym. Test. 26 (4) (2007) 445–450, https://doi.org/10.1016/j.polymertesting.2006.12.011.
[138] G. Shi, S. Araby, C.T. Gibson, Q.S. Meng, S.M. Zhu, J. Ma, Graphene platelets and their polymer composites: fabrication, structure, properties, and applications, Adv. Funct. Mater. 28 (19) (2018), https://doi.org/10.1002/adfm.201706705.
[139] R. Yadav, M. Tirumali, X.G. Wang, M. Naebe, B. Kandasubramanian, Polymer composite for antistatic application in aerospace, Def. Technol. 16 (1) (2020) 107–118, https://doi.org/10.1016/j.dt.2019.04.008.
[140] Z.F. Yang, J.R. Tian, Z.F. Yin, C.J. Cui, W.Z. Qian, F. Wei, Carbon nanotube- and graphene-based nanomaterials and applications in high-voltage supercapacitor: a review, Carbon 141 (2019) 467–480, https://doi.org/10.1016/j.carbon.2018.10.010.
[141] T. Odedairo, J. Ma, Y. Gu, J.L. Chen, X.S. Zhao, Z.H. Zhu, One-pot synthesis of carbon nanotube-graphene hybrids via syngas production, Journal of Materials Chemistry A 2 (5) (2014) 1418–1428, https://doi.org/10.1039/c3ta13871b.
[142] J.A. Oh, Z.G. Yan, S. Araby, R.Y. Wang, H.M. Yu, F. Wei, L. Ming, S.H. Lee, M.J. Alam, M. Jun, Cement nanocomposites containing montmorillonite nanosheets modified with surfactants of various chain lengths, Cement & Concrete Composites 116 (2021), https://doi.org/10.1016/j.cemconcomp.2020.103894.
[143] W. Yu, L. Sisi, Y. Haiyan, L. Jie, Progress in the functional modification of graphene/graphene oxide: a review, RSC Adv. 10 (26) (2020) 15328–15345, https://doi.org/10.1039/d0ra01068e.
[144] M. Gaca, C. Vaulot, M. Maciejewska, M. Lipińska, Preparation and properties of SBR composites containing graphene nanoplatelets modified with pyridinium derivative, Materials 13 (23) (2020) 5407, https://doi.org/10.3390/ma13235407.
[145] E. Maccaferri, L. Mazzocchetti, T. Benelli, A. Zucchelli, L. Giorgini, Morphology, thermal, mechanical properties and ageing of nylon 6,6/graphene nanofibers as Nano(2) materials, Compos. B Eng. 166 (2019) 120–129, https://doi.org/10.1016/j.compositesb.2018.11.096.
[146] X.D. Wang, X.H. Liu, H.Y. Yuan, H. Liu, C.T. Liu, T.X. Li, C. Yan, X.R. Yan, C.Y. Shen, Z.H. Guo, Non-covalently functionalized graphene strengthened poly(vinyl alcohol), Mater. Des. 139 (2018) 372–379, https://doi.org/10.1016/j.matdes.2017.11.023.
[147] M. Naeem, H.C. Kuan, A. Michelmore, Q.S. Meng, A.D. Qiu, M. Aakyiir, D. Losic, S.M. Zhu, J. Ma, A new method for preparation of functionalized graphene and its

epoxy nanocomposites, Compos. B Eng. 196 (2020), https://doi.org/10.1016/j.compositesb.2020.108096.
[148] A. Cruz-Aguilar, D. Navarro-Rodriguez, O. Perez-Camacho, S. Fernandez-Tavizon, C.A. Gallardo-Vega, M. Garcia-Zamora, E.D. Barriga-Castro, High-density polyethylene/graphene oxide nanocomposites prepared via in situ polymerization: morphology, thermal, and electrical properties, Mater. Today Commun. 16 (2018) 232–241, https://doi.org/10.1016/j.mtcomm.2018.06.003.
[149] M. Xiang, C.J. Li, L. Ye, Polyamide 6/reduced graphene oxide nano-composites prepared via reactive melt processing: formation of crystalline/network structure and electrically conductive properties, J. Polym. Res. 26 (5) (2019), https://doi.org/10.1007/s10965-019-1765-x.
[150] M.I. Shueb, M.E. Abd Manaf, C.T. Ratnam, N. Mohamad, M. Mohamed, Enhancement of mechanical and electrical properties in graphene nanoplatelet modified nylon 66, Malaysian J. Compos. Sci. Manufact. 1 (1) (2020) 1–10, https://doi.org/10.37934/mjcsm.1.1.110OpenAccess.
[151] C. Vallés, D.G. Papageorgiou, F. Lin, Z. Li, B.F. Spencer, R.J. Young, I.A. Kinloch, PMMA-grafted graphene nanoplatelets to reinforce the mechanical and thermal properties of PMMA composites, Carbon 157 (2020) 750–760, https://doi.org/10.1016/j.carbon.2019.10.075.
[152] G. Seretis, D. Manolakos, C. Provatidis, On the graphene nanoplatelets reinforcement of extruded high density polyethylene, Compos. B Eng. 145 (2018) 81–89, https://doi.org/10.1016/j.compositesb.2018.03.020.
[153] A. Oyarzabal, A. Cristiano-Tassi, E. Laredo, D. Newman, A. Bello, A. Etxeberría, J.I. Eguiazabal, M. Zubitur, A. Mugica, A.J. Müller, Dielectric, mechanical and transport properties of bisphenol A polycarbonate/graphene nanocomposites prepared by melt blending, J. Appl. Polym. Sci. 134 (13) (2017), https://doi.org/10.1002/app.44654.
[154] S.K. Yeh, C.C. Su, J.M. Huang, M.Q. Ke, D. Bogale, R. Anbarasan, K.L. Tung, S.F. Wang, Fabrication of polystyrene/carbon nanocomposites with superior mechanical properties, Polym. Eng. Sci.. 10.1002/pen.25451.
[155] K. Ka Wei, T.P. Leng, Y.C. Keat, H. Osman, M. Sullivan, V.C. Hong, L.B. Ying, M.S.M. Rasidi, Comparison study: the effect of unmodified and modified graphene nano-platelets (GNP) on the mechanical, thermal, and electrical performance of different types of GNP-filled materials, Polym. Adv. Technol. (2021), https://doi.org/10.1002/pat.5368.
[156] B. Zhao, C. Zhao, M. Hamidinejad, C. Wang, R. Li, S. Wang, K. Yasamin, C.B. Park, Incorporating a microcellular structure into PVDF/graphene–nanoplatelet composites to tune their electrical conductivity and electromagnetic interference shielding properties, J. Mater. Chem. C 6 (38) (2018) 10292–10300, https://doi.org/10.1039/C8TC03714K.
[157] M.R. Zakaria, M.H.A. Kudus, H.M. Akil, M.Z.M. Thirmizir, Comparative study of graphene nanoparticle and multiwall carbon nanotube filled epoxy nanocomposites based on mechanical, thermal and dielectric properties, Compos. B Eng. 119 (2017) 57–66, https://doi.org/10.1016/j.compositesb.2017.03.023.
[158] V. Yadav, P.P. Sharma, A. Rajput, V. Kulshrestha, Aip, thermal and mechanical analysis of PVA/sulfonated carbon nanotubes composite, in: 62nd Dae Solid State Physics Symposium, 2018, https://doi.org/10.1063/1.5028708.
[159] S. Kashyap, S.K. Pratihar, S.K. Behera, Strong and ductile graphene oxide reinforced PVA nanocomposites, J. Alloys Compd. 684 (2016) 254–260, https://doi.org/10.1016/j.jallcom.2016.05.162.
[160] L.M. Bai, N. Bossa, F.S. Qu, J. Winglee, G.B. Li, K. Sun, H. Liang, M.R. Wiesner, Comparison of hydrophilicity and mechanical properties of nanocomposite membranes with cellulose nanocrystals and carbon nanotubes, Environ. Sci. Technol. 51 (1) (2017) 253–262, https://doi.org/10.1021/acs.est.6b04280.
[161] T. Forati, M. Atai, A.M. Rashidi, M. Imani, A. Behnamghader, Physical and mechanical properties of graphene oxide/polyethersulfone nanocomposites, Polym. Adv. Technol. 25 (3) (2014) 322–328, https://doi.org/10.1002/pat.3243.
[162] S. Lin, M.A.S. Anwer, Y.N. Zhou, A. Sinha, L. Carson, H.E. Naguib, Evaluation of the thermal, mechanical and dynamic mechanical characteristics of modified graphite nanoplatelets and graphene oxide high-density polyethylene composites, Compos. B Eng. 132 (2018) 61–68, https://doi.org/10.1016/j.compositesb.2017.08.010.
[163] E. Ivanov, R. Kotsilkova, H.S. Xia, Y.H. Chen, R.K. Donato, K. Donato, A.P. Godoy, R. Di Maio, C. Silvestre, S. Cimmino, V. Angelov, PLA/Graphene/MWCNT composites with improved electrical and thermal properties suitable for FDM 3D printing applications, Appl. Sci. -Basel 9 (6) (2019), https://doi.org/10.3390/app9061209.
[164] E.L. Subtil, J. Goncalves, H.G. Lemos, E.C. Venancio, J.C. Mierzwa, J.d.S. de Souza, W. Alves, P. Le-Clech, Preparation and characterization of a new composite conductive polyethersulfone membrane using polyaniline (PANI) and reduced graphene oxide (rGO), Chem. Eng. J. 390 (2020), 124612, https://doi.org/10.1016/j.cej.2020.124612.
[165] N. Abbas, H.T. Kim, Multi-walled carbon nanotube/polyethersulfone nanocomposites for enhanced electrical conductivity, dielectric properties and efficient electromagnetic interference shielding at low thickness, Macromol. Res. 24 (12) (2016) 1084–1090, https://doi.org/10.1007/s13233-016-4152-z.
[166] N. Bagotia, H. Mohite, N. Tanaliya, D.K. Sharma, A comparative study of electrical, EMI shielding and thermal properties of graphene and multiwalled carbon nanotube filled polystyrene nanocomposites, Polym. Compos. 39 (2018) E1041–E1051, https://doi.org/10.1002/pc.24465.
[167] Z.A. Ghaleb, M. Mariatti, Z.M. Ariff, Synergy effects of graphene and multiwalled carbon nanotubes hybrid system on properties of epoxy nanocomposites, J. Reinforc. Plast. Compos. 36 (9) (2017) 685–695, https://doi.org/10.1177/0731684417692055.
[168] A. Kumar, V. Kumar, M. Kumar, K. Awasthi, Synthesis and characterization of hybrid PANI/MWCNT nanocomposites for EMI applications, Polym. Compos. 39 (11) (2018) 3858–3868, https://doi.org/10.1002/pc.24418.
[169] H. Yazdani, B.E. Smith, K. Hatami, Multi-walled carbon nanotube-filled polyvinyl chloride composites: influence of processing method on dispersion quality, electrical conductivity and mechanical properties, Compos. Appl. Sci. Manuf. 82 (2016) 65–77, https://doi.org/10.1016/j.compositesa.2015.12.005.
[170] Z.B. Wei, Y. Zhao, C. Wang, S. Kuga, Y. Huang, M. Wu, Antistatic PVC-graphene composite through plasticizer-mediated exfoliation of graphite, Chin. J. Polym. Sci. 36 (12) (2018) 1361–1367, https://doi.org/10.1007/s10118-018-2160-5.
[171] G.P. Xiong, P.G. He, Z.P. Lyu, T.F. Chen, B.Y. Huang, L. Chen, T.S. Fisher, Bioinspired leaves-on-branchlet hybrid carbon nanostructure for supercapacitors, Nat. Commun. 9 (2018), https://doi.org/10.1038/s41467-018-03112-3.
[172] M.T. Chen, T. Tao, L. Zhang, W. Gao, C.Z. Li, Highly conductive and stretchable polymer composites based on graphene/MWCNT network, Chemical Communications 49 (16) (2013) 1612–1614, https://doi.org/10.1039/c2cc38290c.
[173] X.M. Liang, Q.F. Cheng, Synergistic reinforcing effect from graphene and carbon nanotubes, Composites Communications 10 (2018) 122–128, https://doi.org/10.1016/j.coco.2018.09.002.
[174] P.A. Song, L.N. Liu, S.Y. Fu, Y.M. Yu, C.D. Jin, Q. Wu, Y. Zhang, Q. Li, Striking multiple synergies created by combining reduced graphene oxides and carbon nanotubes for polymer nanocomposites, Nanotechnology 24 (12) (2013), https://doi.org/10.1088/0957-4484/24/12/125704.
[175] S. Mondal, D. Khastgir, Elastomer reinforcement by graphene nanoplatelets and synergistic improvements of electrical and mechanical properties of composites by hybrid nano fillers of graphene-carbon black & graphene-MWCNT, Compos. Appl. Sci. Manuf. 102 (2017) 154–165, https://doi.org/10.1016/j.compositesa.2017.08.003.
[176] S. Chatterjee, F. Nafezarefi, N.H. Tai, L. Schlagenhauf, F.A. Nuesch, B.T.T. Chu, Size and synergy effects of nanofiller hybrids including graphene nanoplatelets and carbon nanotubes in mechanical properties of epoxy composites, Carbon 50 (15) (2012) 5380–5386, https://doi.org/10.1016/j.carbon.2012.07.021.
[177] W.K. Li, A. Dichiara, J.B. Bai, Carbon nanotube-graphene nanoplatelet hybrids as high-performance multifunctional reinforcements in epoxy composites, Compos. Sci. Technol. 74 (2013) 221–227, https://doi.org/10.1016/j.compscitech.2012.11.015.
[178] M.K. Shukla, K. Sharma, Effect of functionalized graphene/CNT ratio on the synergetic enhancement of mechanical and thermal properties of epoxy hybrid composite, Mater. Res. Express 6 (8) (2019), 085318, https://doi.org/10.1088/2053-1591/ab1cc2.
[179] M. Verma, S.S. Chauhan, S. Dhawan, V. Choudhary, Graphene nanoplatelets/carbon nanotubes/polyurethane composites as efficient shield against electromagnetic polluting radiations, Compos. B Eng. 120 (2017) 118–127, https://doi.org/10.1016/j.compositesb.2017.03.068.
[180] H.M. Zhang, G.C. Zhang, M. Tang, L.S. Zhou, J.T. Li, X. Fan, X.T. Shi, J.B. Qin, Synergistic effect of carbon nanotube and graphene nanoplates on the mechanical, electrical and electromagnetic interference shielding properties of polymer composites and polymer composite foams, Chem. Eng. J. 353 (2018) 381–393, https://doi.org/10.1016/j.cej.2018.07.144.
[181] L. Yue, G. Pircheraghi, S.A. Monemian, I. Manas-Zloczower, Epoxy composites with carbon nanotubes and graphene nanoplatelets - dispersion and synergy effects, Carbon 78 (2014) 268–278, https://doi.org/10.1016/j.carbon.2014.07.003.
[182] A. Li, C. Zhang, Y.-F. Zhang, Thermal conductivity of graphene-polymer composites: mechanisms, properties, and applications, Polymers 9 (9) (2017) 437, https://doi.org/10.3390/polym9090437.